Environmental and Sustainability Indicators 30 (2026) 101254

Contents lists available at ScienceDirect

Environmental and Sustainability Indicators

journal homepage: www.sciencedirect.com/journal/environmental-and-sustainability-indicators

Integrating artificial and collective intelligence in hydro-economic modeling for sustainable irrigation and drought adaptation in Colombia

Sonia Mercedes Polo-Murcia [a,*], Marta García-Mollá [b], César Augusto Terán-Chaves [c]

[a] PhD Program in Agri-Food Economics.Universitat Politécnica de Valencia, 46022, Valencia, Spain
[b] Valencian Centre for Irrigation Studies (CVER), Universitat Politécnica de Valencia, 46022, Valencia, Spain
[c] Grupo de Investigación Agricultura Inteligente Para la Sostenibilidad de los Sistemas de Producción en el Trópico, Universidad Nacional de Colombia, 111321, Bogotá D. C., Colombia

ARTICLE INFO

Keywords:
AquaCrop
Bayesian inference
Decision support system
Dirichlet posterior
Food security
Machine-learning surrogate

ABSTRACT

Water-scarce smallholder regions require irrigation strategies that are both biophysically credible and socially legitimate. We propose an integrated hydro-economic decision-support framework for the Cesar Department (Colombia) that couples (i) AI emulation of FAO AquaCrop crop–water responses, (ii) Bayesian aggregation of collective intelligence elicited under Shared Socioeconomic Pathways (SSP) using an AHP-anchored, two-round Delphi protocol, and (iii) a household linear program enforcing diversification and a Top-M social-alignment rule with penalized slack. XGBoost surrogates generate household-specific yield and net irrigation requirement coefficients for four crops under a dry-year baseline (test R^2: 0.89–0.93 for yield; 0.87–0.91 for NIR). Expert-derived SSP-specific crop priority vectors are modeled on the simplex and combined via a Dirichlet posterior to produce crop-preference weights with 95% credible intervals, operationalized as social-weight layers (Base/Low/High/Uniform/Favored). The model solves 2520 household–scenario combinations (168 households × 3 SSPs × 5 layers) with full feasibility and zero slack use. Increasing normative leverage through the minimum-alignment quota (α) and social-reward scaling (μ) raises the social welfare component with limited income disruption in SSP1 and SSP4: in SSP4, the mean objective increases from USD 8334 (Base) to USD 11,427 (Favored), driven by the social term (USD 3283 → 6382) while net income remains stable (~USD 5045–5052). SSP3 provides a stress test, revealing tighter feasibility (alignment 0.582 and net income USD 3661 under Low; binding rate 22%). Across Socioeconomic Vulnerability Index (SEVI) terciles, mean income declines by ~42% while alignment remains high, motivating complementary investments that relax constraints for high-vulnerability households. Overall, embedding uncertainty-aware social priorities into hydro-economic optimization enables policy-relevant, scenario-conditional irrigation guidance while transparently revealing when preference-consistent targeting is compatible with feasibility and when it requires enabling investments.

1. Introduction

Water scarcity and climate variability have increasingly constrained agricultural livelihoods in semi-arid regions, where irrigation-dependent farming systems remain highly sensitive to hydrological uncertainty and seasonal rainfall variability. These pressures are especially acute in river basins with limited storage capacity, strong intra-annual climate variability, and competing water demands, where smallholder agriculture often experiences elevated exposure to drought risk and income instability. Responding to these challenges requires analytical frameworks that can explicitly link hydrological processes, crop production responses, economic decision-making, and social vulnerability under climate stress.

Hydro-economic models have provided a rigorous foundation for evaluating water-allocation trade-offs by integrating hydrological representations with economic optimization (Cai et al., 2002; Harou et al., 2009). Their evolution has expanded toward multi-sectoral integration, salinity–water interactions, and policy analysis in irrigation-dependent systems (Blanco-Gutiérrez et al., 2013; Zhou et al., 2023; Cao et al., 2024), with recent applications assessing climate-change impacts and adaptation strategies (Esteve et al., 2015) and quantifying the economic value of water across competing uses (Crespo et al., 2025). Despite these advances, many hydro-economic approaches remain predominantly technocratic: stakeholder priorities are often weakly represented, and

* Corresponding author.
E-mail addresses: smpolmur@upv.edu.es (S.M. Polo-Murcia), mgarmo@esp.upv.es (M. García-Mollá), cesar.teran1@outlook.com (C.A. Terán-Chaves).

https://doi.org/10.1016/j.indic.2026.101254
Received 12 February 2026; Received in revised form 20 March 2026; Accepted 6 April 2026
Available online 9 April 2026

equity, distributional outcomes, and household-level vulnerability remain insufficiently resolved (Eamen et al., 2022; Ward, 2024). As a result, models may identify solutions that are optimal in aggregate terms but misaligned with locally salient priorities or differential capacity to adapt. Recent efforts have begun to bridge this gap by coupling hydrological simulation with multi-criteria decision frameworks and climate scenarios to support crop selection and agricultural planning under water scarcity (Javan and Darestani, 2024); however, stakeholder-derived priorities in such frameworks typically enter as fixed expert scores rather than as probabilistic inputs whose uncertainty is formally propagated through the optimization, limiting their ability to reflect the contested and context-dependent nature of collective preferences.

A central determinant of model credibility in coupled water–agriculture systems is the representation of crop yield responses to water availability. Process-based crop models such as APSIM (Holzworth et al., 2014), AquaCrop (Raes et al., 2009, 2018; Foster et al., 2017), DSSAT (Jones et al., 2003), EPIC (Williams et al., 1989) and WOFOST (De Wit et al., 2018) have been widely used to simulate crop growth under varying climatic and management conditions. Among these, AquaCrop has been particularly relevant in data-scarce and water-limited environments because of its parsimonious structure, explicit focus on water productivity, and comparatively low data requirements (Raes et al., 2009). Artificial intelligence approaches have demonstrated complementary value in this context: machine-learning models trained on climate and hydrological data can capture nonlinear discharge responses to temperature and precipitation variability in semi-arid basins, providing computationally efficient surrogates for complex process-based simulations (Javan et al., 2015). Recent algorithmic enhancements and integrations with real-time monitoring and forecasting have further strengthened its applicability for adaptive irrigation management and scenario analysis (Sharafi et al., 2023; Puig et al., 2025). However, embedding crop-model realism within decision frameworks that remain computationally tractable at household scale continues to be a practical challenge.

In Colombia, emerging multi-model frameworks that couple land suitability analysis, surface-water availability assessment, and crop–water simulation have demonstrated the value of bridging biophysical and socio-economic dimensions to support irrigation planning under climate variability (Polo-Murcia et al., 2025). Complementary participatory research has also shown that technically optimal strategies may fail in practice if they are not aligned with local priorities, institutional constraints, and perceived vulnerability (Polo-Murcia et al., 2025). Yet, few modeling systems have operationalized a fully integrated decision-support architecture that jointly (i) predicts crop–water responses at scale, (ii) optimizes household allocations under hydrological constraints, and (iii) embeds participatory governance signals—while explicitly acknowledging uncertainty in those signals.

As emphasized by Razavi et al. (2025), a key frontier in human–water systems modeling lies in convergent, transdisciplinary approaches that unify biophysical, economic, and social dimensions while remaining operationally relevant for decision-makers. In response, this study developed an AI-assisted hydro-economic framework in which surrogate models trained on extensive AquaCrop simulations provided household-specific crop–water response coefficients, and an optimization engine allocated land and irrigation water under scarcity while explicitly incorporating community-defined priorities. The predictive layer enhanced computational efficiency and enabled rapid exploration of climate–water scenarios, whereas the participatory layer embedded locally derived vulnerability and resilience considerations into allocation strategies.

The Cesar department in northern Colombia provided a pertinent testing ground. Characterized by pronounced hydroclimatic variability, limited water-storage infrastructure, and strong dependence on irrigation for rural livelihoods, the basin represented a critical case for examining how integrated modeling approaches could inform equitable and adaptive water-management strategies in semi-arid contexts. By combining machine-learning prediction, hydro-economic optimization, and participatory preference weighting, this research advanced a socially informed and adaptive paradigm for water governance, illustrating how artificial intelligence could complement collective intelligence to support more resilient, context-responsive irrigation planning.

Accordingly, this study aimed to: (i) develop an AI-assisted hydro-economic model linking crop–water responses with household-level land and water allocation decisions; (ii) integrate stakeholder-defined priorities, elicited through the SSP–AHP framework, into the optimization logic; and (iii) assess distributional and vulnerability-differentiated outcomes under contrasting socio-institutional futures in the Cesar Department.

2. Materials and methods

2.1. Study framework and conceptual approach

This study develops an integrated hydro-economic decision-support framework for resource-constrained smallholder irrigation under water scarcity and climatic uncertainty. It couples (i) household-specific crop–water response coefficients produced by machine-learning surrogates calibrated to FAO AquaCrop simulations, (ii) a participatory pipeline that elicits adaptation priorities under alternative Shared Socioeconomic Pathways (SSP) and translates them into crop social weights, and (iii) a household linear program (LP) that allocates land, water, labor, and capital while maximizing net income augmented by an explicit social-value term (Fig. 1).

The methodological novelty is to embed collective priorities as uncertainty-aware, testable constraints within optimization. Bayesian social weights are implemented through a Top-*M* alignment rule, with a penalized slack variable that preserves feasibility when binding constraints prevent full compliance. This turns normative steering into an auditable, constraint-aware mechanism that can be stress-tested across SSP, revealing shifts in welfare composition, feasibility, and crop portfolios. Model parameters, symbols, units, baseline values, and provenance are reported in Table S1.

Critically, this auditability rests on the joint use of two elements that prior MCDM-informed hydro-economic models have only rarely combined: a Dirichlet posterior that represents elicited crop priorities as a full probability distribution on the simplex, rather than as a fixed point estimate; and a Top-M alignment rule that translates that distributional output into a binding, operational allocation rule. Each element alone is insufficient: the posterior without the alignment rule leaves uncertainty disconnected from allocation, whereas the alignment rule without the posterior reduces normative steering to a deterministic priority signal.

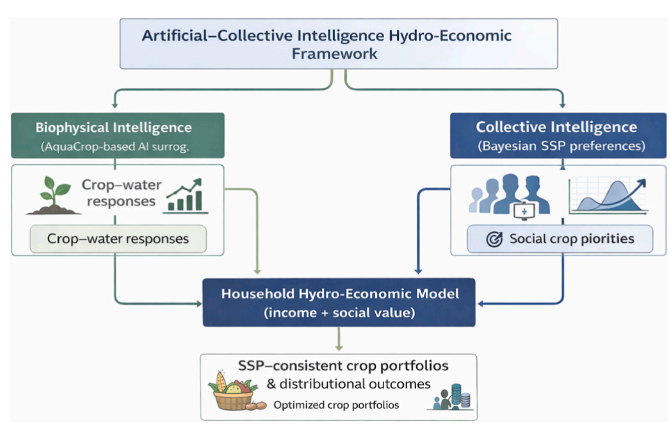

Fig. 1. Conceptual architecture of an artificial–collective intelligence hydro-economic framework for irrigation under drought.

Their combination is what makes collective priorities simultaneously probabilistic, operational, and feasibility-testable across SSP scenarios.

In this sense, the contribution goes beyond the use of stakeholder-derived weights per se and lies in converting uncertainty-aware social priorities into allocative implications that can be evaluated under real household resource constraints.

2.2. Study area and household dataset

The empirical application is the Cesar Department, Colombia (Colombian Caribbean; 07°41′16″–10°52′14″ N, 72°53′27″–74°08′28″ W), covering ~22,905 km^2 and characterized by strong hydroclimatic seasonality and recurrent dry-season low-flow constraints on irrigation. Irrigation is predominantly self-managed; thus, scarcity is represented as household-accessible water rather than legally assigned volumetric rights.

Household data were collected through a standardized survey conducted between June and August 2024 (Polo-Murcia et al., 2026). Sampling followed a stratified random design with proportional allocation across five ecoregions using the national census sampling frame (DANE. Departamento Nacional de Estadísticas, 2014) and a finite-population sample size computed using Yamane's formula (Yamane, 1973). Territorial statistics from Colombia's National Agricultural Census (DANE. Departamento Nacional de Estadísticas, 2014) were used to contextualize irrigation prevalence and technology types (e.g., pumping vs. gravity/manual systems), supporting parameterization where engineering inventories are unavailable.

Households constitute the decision units $h = 1,\ldots,H$, with $H = 168$. Spatial heterogeneity is represented by the municipality index $m(h)$. The crop set is $K = \{\text{maize}, \text{rice}, \text{beans}, \text{cassava}\}$. Each household chooses among feasible crop–management options (k,i), where $i \in I_h(k)$ denotes the set of options available for crop k at household h.

Throughout the manuscript, cycle denotes the crop growing period (i.e., the time from planting to harvest) used to express all per-cycle quantities (labor, costs, irrigation depth, and water accessibility). In the Cesar case study, we adopt crop-specific cycle lengths consistent with local agronomic calendars.

2.3. Biophysical module: crop–water response generation

Household-specific biophysical coefficients were generated using machine-learning surrogates trained on a pre-existing, spatially distributed FAO AquaCrop simulation dataset for the four target crops under multiple irrigation regimes (Polo-Murcia et al., 2025). The underlying simulations were run at 1009 locations parameterized with local soil conditions, producing paired inputs (climate, soil, management) and outputs (yield and net irrigation requirement, NIR). Climate forcing was based on a published dry-year Typical Meteorological Year (TMY) for the Cesar Department, derived using the TMY–precipitation deficit approach from long-term station records (Domínguez et al., 2013; Terán-Chaves et al., 2023). This dry-year TMY product was adopted directly to ensure full consistency with the Cesar Department wide scarcity characterization applied across the framework.

Extreme Gradient Boosting (XGBoost) models were trained to emulate AquaCrop's input–output mapping, using simulation features as predictors and simulated yield and NIR as targets. Ensemble learning approaches have shown strong fidelity in reproducing AquaCrop responses while reducing computational burden (Batool et al., 2022; Chumbe et al., 2023; Zhang et al., 2024; Ramesh and Kumaresan, 2025).

Household coordinates were linked to the same climate and soil raster datasets used to parameterize the original simulations, constructing environmentally analogous feature vectors. The trained surrogates then produced option-level predictions: yield $\widehat{Y}_{hki}$ (t ha^{-1}) and net irrigation requirement $\widehat{NIR}_{hki}$ (mm cycle^{-1}) for each feasible (h,k,i). These coefficients are subsequently embedded into the optimization model.

2.4. Collective intelligence: participatory elicitation and bayesian inference of ssp-specific social weights

This subsection converts stakeholder deliberation and expert judgment into SSP-conditional crop social weights $w_{s,k,g}$ that can be used directly by the hydro-economic optimization model (Section 2.5). As summarized in Fig. 2, the workflow proceeds from (i) participatory identification of SSP-dominant adaptation strategies, to (ii) translation into measurable crop-evaluation criteria, to (iii) structured expert scoring, and (iv) Bayesian Dirichlet aggregation to obtain a posterior distribution of crop priorities and its uncertainty, which is then propagated through a set of social-weight layers.

2.4.1. Participatory identification of SSP-dominant strategies and crop-evaluation criteria

To ground preference elicitation in plausible future conditions, we framed the analysis around three Shared Socioeconomic Pathways (SSP), SP1 (Sustainability), SSP3 (Regional Rivalry), and SSP4 (Inequality). The SSP framework provides internally consistent narratives of socioeconomic development and governance conditions that shape adaptation challenges and opportunities (O'Neill et al., 2017). Following established approaches for contextualizing SSPs in water-governance and irrigation planning (Ortega-Reig et al., 2019), we

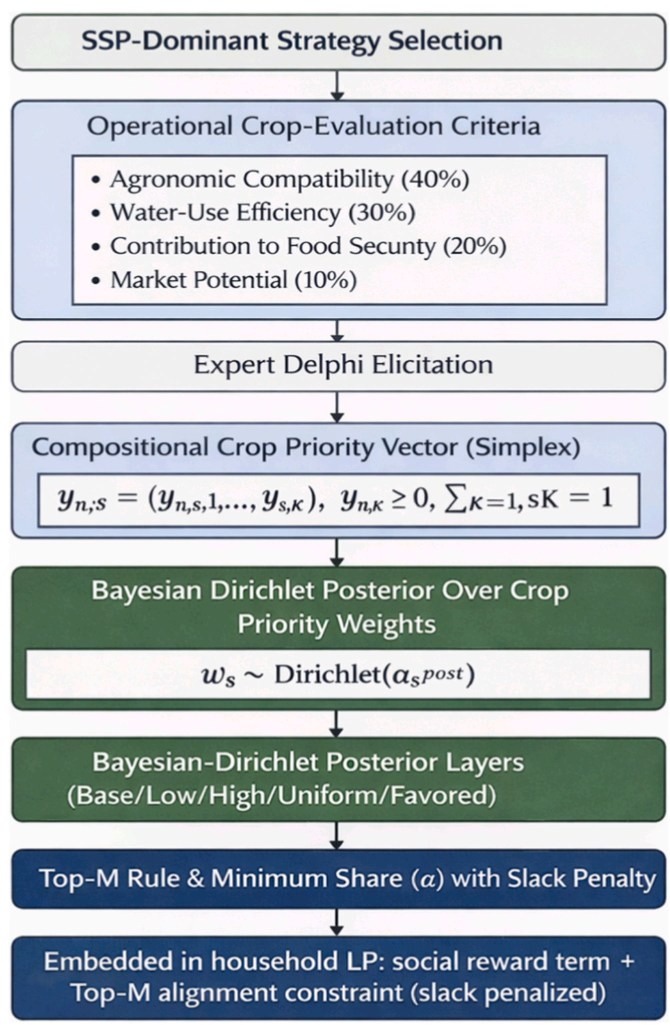

Fig. 2. Workflow of collective intelligence elicitation and bayesian inference of SSP-specific crop priorities.

tailored these narratives to locally plausible governance and market settings in the Department of Cesar to anchor participatory deliberation. Stakeholder priorities were then elicited using the Analytic Hierarchy Process (AHP) in participatory workshops previously conducted in the study area (Polo-Murcia et al., 2026).

SSP1, SSP3, and SSP4 were selected because they represent contrasting yet locally plausible governance–adaptation archetypes for the Cesar smallholder irrigation context. The aim was not to span the full SSP family, but to stress-test the framework under divergent social-priority regimes with marked differences in institutional coordination, market access, and adaptive capacity. SSP2 was not included because the study did not seek a middle-of-the-road baseline; rather, it prioritized scenarios with stronger social and institutional contrast for evaluating the model's response. SSP5 was also excluded because its high-growth, fossil-fueled development logic was considered less representative of the resource-constrained smallholder context examined here and therefore less informative for the specific policy questions addressed by the model.

A total of 18 stakeholders evaluated four adaptation strategies via pairwise comparisons across four criteria: Technical and Economic Viability, Community Acceptance, Climate Resilience, and Territorial Equity. For each SSP, the adaptation strategy with the highest normalized AHP priority was selected as the SSP-dominant strategy (Table 1). This dominant strategy then serves as the scenario anchor for the next step: translating collective priorities into SSP-specific crop-preference weights, so that crop portfolios—maize, rice, beans, and cassava—remain consistent with the adaptation logic implied by each SSP narrative.

Each SSP-dominant strategy was translated into a common set of four crop-evaluation criteria—Agronomic Compatibility, Water-Use Efficiency, Contribution to Food Security, and Market Potential—drawing on MCDA frameworks for agricultural resource management under water scarcity (Hayashi, 2000; Psomas et al., 2018; Radmehr et al., 2022; Abdolalizadeh et al., 2025). These four criteria reflect dimensions consistently identified as central in multi-criteria assessments of irrigated crop systems: agronomic and technological suitability under local conditions, water productivity and efficient use under scarcity constraints, food production contribution and household-level viability, and economic return through market access. The operational definitions and fixed criterion weights used to assess crop–strategy alignment are reported in Table 2. These criteria and weights were reviewed and refined through a modified Delphi process to ensure clarity, relevance, and consistency with the earlier AHP criteria. To quantify crop alignment under each SSP, a panel of twelve independent experts scored each crop on a 0–1 scale for each criterion, using a two-round elicitation protocol with anonymized feedback between rounds (Hemming et al., 2018a,b). For each expert n and SSP s, criterion-weighted crop scores were aggregated and then normalized to the simplex to obtain an SSP-specific crop-priority vector:

Table 1
Dominant AHP-derived adaptation strategies per SSP (adapted from Polo-Murcia et al., 2026).

SSP Scenario	Dominant Strategy	Priority Weight (%)	Primary Rationale
SSP1	Climate-Resilient Food Production with Efficient Irrigation	38	Balances food security with water sustainability under green development
SSP3	Decentralized Rainwater Harvesting	38	Fits fragmented, self-reliant futures with limited institutional support
SSP4	Fair Market Access and Cooperative Marketing Platforms	47	Addresses structural inequalities in market access and value chains

Table 2
Operational criteria and weights for evaluating crop–strategy alignment in the Scenario-Conditioned Crop Matching (SCCM) module.

Criterion (Weight)	Operational Definition	Theoretical Basis & Link to AHP Criteria
Agronomic Compatibility (40%)	Degree to which standard cultivation practices and physiological requirements align with the strategy's core agronomic principles (e.g., suitability for deficit irrigation, soil conservation compatibility).	Primary feasibility filter; links to Climate Resilience (CR) and Technical Viability (VTE) from AHP. Extends criteria used in irrigation planning AHP applications (Montazar and Gaffari, 2011).
Water-Use Efficiency (30%)	Crop's water productivity (yield per unit water consumed) under the water management regime implied by the strategy, considering both blue and green water components.	Central to water-scarce basins; directly underpins Climate Resilience (CR) and resource-related VTE from AHP. Corresponds to water-related criteria in irrigation AHP models (Montazar and Gaffari, 2011).
Contribution to Food Security (20%)	Relative importance for household nutrition (calorie and protein provision) and dietary diversity under SSP-specific socioeconomic conditions.	Captures social dimensions; aligns with Community Acceptance (AC) and Territorial Equity (TE) from AHP.
Market Potential (10%)	Viability within formal/informal market structures anticipated under the SSP, considering projected demand, price stability, and value chain access across socioeconomic groups.	Represents economic linkage; connects to income-related aspects of VTE and AC from AHP.

$$\mathbf{y}_{n,s} = \left(y_{n,s,1}, \ldots, y_{n,s,K}\right), y_{n,s,k} \geq 0, \sum_{k=1}^{K} y_{n,s,k} = 1. \tag{1}$$

The vector $\mathrm{y}_{n,s}$ is interpreted as a relative crop-priority share (alignment-based) under SSP s.

The Delphi protocol yielded, for each expert n and SSP s, a criterion-weighted and normalized crop-priority composition $y_{n,s}$. We then aggregated these compositions under a Dirichlet framework to obtain SSP-specific priority weights w_s with explicit uncertainty.

The expert panel comprised twelve Colombian scientists with demonstrated expertise in agronomy, hydrology, agricultural economics, and rural development policy, all with direct territorial knowledge of the Cesar Department (mean experience ≥10 years; see Table S2 in Supplementary Material). The 18 stakeholders who participated in the prior AHP workshops were drawn from the study area and included smallholder water users, community leaders, and local government representatives (Polo-Murcia et al., 2026; Table S2).

2.4.2. Dirichlet posterior inference for SSP-specific crop priority weights

To obtain SSP-specific crop-priority weights while propagating inter-expert dispersion, we treated each expert's SSP-conditioned judgments as a compositional vector on the simplex. From the consolidated expert score file, criterion scores were aggregated into a crop-level weighted score per expert n, SSP s, and crop k using analyst-defined criterion weights, and then normalized so that each expert's crop priorities sum to one ($y_{n,s,k} \geq 0$ and $\sum_k y_{n,s,k} = 1$). A small lower bound was applied in the implementation to avoid zero entries before normalization.

Uncertainty over SSP-specific crop-priority shares was modeled using a Dirichlet distribution, appropriate for simplex-valued vectors and commonly used to represent uncertainty in compositional judgments in structured elicitation settings (Wilson et al., 2021). We adopted a weakly informative prior α_0 (default symmetric $\alpha_{0,k} = 1$ if no crop-specific values are supplied). To reflect heterogeneous internal consistency across experts, each expert contribution was scaled by a reliability-derived concentration weight κ, computed from the analyst-provided consistency metric, rescaled within each SSP, and bounded to avoid extreme influence (details in Appendix 1).

The SSP-specific posterior concentration vector was constructed as:

$$\alpha_s^{post} = \alpha_0 + \sum_{n=1}^{N} \kappa_{n,s}\, y_{n,s} \tag{2}$$

where s indexes the SSP scenario; $\alpha_s^{post} \in \mathbb{R}_+^K$ is the SSP-specific Dirichlet posterior concentration vector over the K crops; $\alpha_0 \in \mathbb{R}_+^K$ is the Dirichlet prior concentration vector (default $\alpha_{0,k} = 1\ \forall k$ if not specified); $n = 1, \dots, N$ indexes experts and N is the number of experts available for SSP s; $\kappa_{n,s} \in \mathbb{R}_+$ is the reliability (effective concentration) weight assigned to expert n under SSP s (computed from the expert's consistency metric and rescaled within SSP); and $y_{n,s} \in \Delta^{K-1}$ is expert n's SSP-specific crop-priority composition on the simplex, with elements $y_{n,s,k} \geq 0$ and $\sum_{k=1}^{K} y_{n,s,k} = 1$.

Posterior draws of the SSP-specific crop-priority vector w_s were then obtained as:

$$w_s \Big| \left\{ y_{n,s} \right\}_{n=1}^{N} \sim \text{Dirichlet}\left(\alpha_s^{post}\right) \tag{3}$$

For each SSP, we generated Monte Carlo draws from this posterior and summarized $w_{s,k}$ using posterior means and 95% credible intervals, yielding SSP-specific crop-priority weights as probabilistic inputs suitable for robustness-aware interpretation (Yet and Tuncer Şakar, 2020; Wilson et al., 2021).

Robustness and consensus classification. To quantify ranking stability in a diversification-relevant way, we computed p_{top2}, the posterior probability that a crop appears among the Top-2 crops across draws. Using pre-defined thresholds on p_{top2}, each crop–SSP combination was classified as: High Consensus ($p_{\text{top2}} \geq 0.80$), Moderate Consensus ($0.60 \leq p_{\text{top2}} < 0.80$), or High Controversy ($p_{\text{top2}} < 0.60$).

2.4.3. *Construction of SSP-specific social-weight layers for hydro-economic analysis*

The Dirichlet posterior from Section 2.4.2 yields, for each SSP s, a crop-priority vector $w_s = (w_{s,1}, \dots, w_{s,K})$ that represents the relative social priority assigned to each crop. To translate this posterior information into inputs useable by the hydro-economic LP, we define a set of social-weight layers $g \in G$.

In practical terms, each layer is simply a numerical score vector over crops:

$w_{s,g} = (w_{s,1,g}, \dots, w_{s,K,g}), w_{s,k,g} \geq 0, \sum_{k=1}^{K} w_{s,k,g} = 1,$ So it can be directly embedded in the optimization model as the normative weights that (i) parameterize the social-value term and (ii) determine the SSP-preferred set used by the Top-M alignment rule. These weights are not observed probabilities and not ordinal ranks; they are normalized, scenario-specific priority scores derived from the elicitation and posterior inference.

We construct five SSP-specific social-weight layers $g \in \{\text{Base}, \text{Low}, \text{High}, \text{Uniform}, \text{Favored}\}$, each defined as a crop-weight vector $w_{s,\cdot,g}$ constrained to the simplex $\left(w_{s,k,g} \geq 0, \sum_k w_{s,k,g} = 1\right)$ and therefore directly embeddable in the hydro-economic LP (Table 3). This compact set isolates the role of normative priorities from biophysical–economic drivers and enables sensitivity analysis to both preference uncertainty and policy-anchored prioritization. The Base layer uses the posterior mean $E[w_{s,k}|\text{data}]$ and serves as the default specification for the core results. The Low and High layers rely on the 2.5% and 97.5% posterior credible bounds (renormalized within each SSP), representing conservative and optimistic realizations of collective priorities. The Uniform layer assigns equal weights $1/K$ to all crops and provides a neutral benchmark against which the added value of incorporating social preferences can be assessed.

Table 3
Bayesian-derived social preference layers and normative scenarios (social-weight layers) embedded in the hydro-economic LP (by SSP).

Layer (g)	Definition of $w_{s,k,g}$ (for crop k under SSP s)	Interpretation
Base	$w_{s,k,\text{Base}} = \mathbb{E}[w_{s,k}\|\text{data}]$	Central collective-preference estimate.
Low	$w_{s,k,\text{Low}} = \text{Norm}(Q_{0.025}[w_{s,k}\|\text{data}])$	Conservative realization of collective preferences.
High	$w_{s,k,\text{High}} = \text{Norm}(Q_{0.975}[w_{s,k}\|\text{data}])$	Optimistic realization of collective preferences.
Uniform	$w_{s,k,\text{Uniform}} = 1/K$	No crop prioritization (neutral benchmark).
Favored	$w_{s,k,\text{Favored}} = \text{Norm}(q_{s,k})$	SSP-consistent ex-ante prioritization (normative; not posterior-derived).

Notes: $\text{Norm}(x_k) = x_k / \sum_{j=1}^{K} x_j$. All layers satisfy $w_{s,k,g} \geq 0$ and $\sum_{k=1}^{K} w_{s,k,g} = 1$ for each SSP s and layer g. For the Favored layer, the SSP-specific ex-ante scores $q_{s,k}$ are: SSP1 (rice 0.50, maize 0.25, beans 0.15, cassava 0.10); SSP3 (cassava 0.45, beans 0.30, maize 0.15, rice 0.10); SSP4 (maize 0.40, rice 0.30, beans 0.20, cassava 0.10). These values define an author-defined, SSP-consistent what-if stress-test scenario. They are specified a priori, are not inferred from the posterior, and are used only to test model sensitivity to a strong directed policy signal. They should not be interpreted as empirical outputs of the collective-intelligence process or as policy targets.

The Favored layer is a normative, SSP-consistent policy stress test defined independently of the posterior (Table 3). It operationalizes the adaptation logic implied by each SSP narrative and the corresponding SSP-dominant strategy described in Section 2.4.1 by assigning SSP-specific ex ante crop scores $q_{s,k}$, which are then normalized as $w_{s,k}^{Fav} = q_{s,k} / \sum_j q_{s,j}$. Unlike the posterior-derived layers, the Favored layer is not inferred from stakeholder data or from the collective intelligence process. Instead, it is an author-defined what-if scenario in which the ex ante scores are specified a priori to assign a deliberately higher priority weight to the crop most consistent with the dominant adaptation logic of each SSP, while maintaining positive weights for all crops and preserving simplex validity. Accordingly, SSP1 emphasizes sustainability-oriented staples (rice and maize), SSP3 prioritizes resilient subsistence crops under constrained conditions (cassava and beans), and SSP4 emphasizes market-oriented staples consistent with unequal access and differentiated returns (maize and rice). The Favored layer is therefore used only to test model sensitivity to a strong directed policy signal and should not be interpreted as a posterior result or as a normative policy target.

2.4.4. *Operational parameterization linked to SSP narratives*

The weights $w_{s,k,g}$ become actionable in the LP through a small set of scenario-specific policy levers—the minimum alignment share $\alpha_{s,g}$, the social reward intensity $\mu_{s,g}$, and the Top-M size used to define the prioritized crop set $M_{s,g}$. The values of α, μ, and Top-M are reported transparently in Table S3 and are calibrated to remain consistent with SSP narratives and preliminary sensitivity checks. The next subsection (Section 2.5) specifies the LP and shows exactly how $w_{s,k,g}$, $\alpha_{s,g}$, $\mu_{s,g}$, and $M_{s,g}$ enter the optimization.

2.5. *Hydro-economic optimization model and scenario design*

Building on the SSP-specific inference, we translate collective priorities into scenario- and layer-specific crop social weights $w_{s,k,g}$, which provide a reproducible numeric representation of stakeholder preferences and their uncertainty. This section introduces the household hydro-economic linear program (LP) and explains how $w_{s,k,g}$ is operationalized in two complementary ways: (i) as an additive social premium in the objective function, and (ii) as a minimum alignment requirement defined over the scenario-specific Top-M crop set $M_{s,g}$. The model is solved subject to binding household constraints on land, water, labor, and budget. Before detailing the equations, Table 4 summarizes the indices/sets, decision variables, biophysical and economic coefficients, endowments, and social-alignment parameters used in the LP.

Fig. 3 provides an overview of the run sequence for each household h, SSP scenario s, and social-weight layer g. It highlights where the SSP-specific weights enter the LP (objective and alignment constraint) and how cases of infeasible alignment are tracked using a slack variable that is penalized in the objective function.

2.5.1. Hydrologic scarcity, irrigation-water cost accounting

Hydrologic scarcity and household-accessible water. Municipality low-flow conditions are represented by $Q90_{m,s}$ (flow exceeded 90% of the time) derived from flow-duration curves (Polo-Murcia et al., 2025). Water accounting uses the standard depth–volume conversion:

$$1mm\ over\ 1\ ha = 10m^3 \tag{4}$$

Household-accessible irrigation water per cycle is defined as:

$$W^{acc}_{h,s} = \phi_h\ T\left(Q90_{m(h),s}\right) \tag{5}$$

where $W^{acc}_{h,s}$ is expressed in mm·ha per cycle, $\phi_h \in (0,1]$ is a household accessibility multiplier, and $T(\cdot)$ converts $Q90$ from L s^{-1} ha^{-1} to mm·ha per cycle using standard flow-to-volume conversions and Eq. (4). The baseline specification sets $\phi_h = 1$.

Irrigation feasibility and marginal water cost. We represent irrigation costs through a linear marginal cost of applied water (USD m^3) combining volumetric charges and pumping/energy costs:

$$c^{water}_h = \frac{\text{Tariff}_{(\text{COP/m}^3)}}{\text{COP per USD}} + \left(\frac{\text{Energy}_{(\text{COP/kWh})}}{\text{COP per USD}}\right) \times \left(\text{kWh per m}^3\right) \tag{6}$$

Using Eq. (4), the per-hectare irrigation cost per cycle for option (h,k,i) is:

$$C^{water}_{hki} = c^{water}_h \times 10 \times GIR_{hki}\left(\text{USD ha}^{-1}\text{cycle}^{-1}\right) \tag{7}$$

where GIR_{hki} is the gross irrigation requirement (mm cycle^{-1}), computed as $GIR_{hki} = \widehat{NIR}_{hki}/\eta$, with η denoting application efficiency. Global conversion factors and unit values used in water-cost accounting are reported in Table S4.

2.5.2. Household linear programming model: decision variables, objective, and standard constraints

We model each household's crop-allocation decision as an LP. Let $h = 1,\dots,H$ index households, $k \in K$ crops, and $i \in I_h(k)$ feasible management options for crop k at household h. The main decision variable is cultivated area A_{hki} (ha). The model also allows hired labor H_h (labor-days per cycle) and includes a slack S_h (ha) to preserve feasibility of the social-alignment rule.

Non-negativity and decision space.

$$A_{hki} \geq 0\ \ \forall k \in K, i \in I_h(k), H_h \geq 0, S_h \geq 0 \tag{8}$$

For each household h, SSP s, and social-weight layer g, the LP maximizes:

where H_h is hired labor (days) and S_h is a slack variable used to preserve feasibility of the social-alignment rule (Section 2.5.3). Eq. (8) defines the optimization decision space for each (h,s,g).

Objective function. For each household h, SSP s, and social-weight layer g, the LP maximizes:

$$Max \sum_{k\,\epsilon\,K} \sum_{i\,\epsilon\,I_h(k)} \left[\pi_{h\,k\,i} - C^{water}_{hki} + \mu^{eff}_{s,g}\, w_{s,k,g}\right] A_{hki} - w^{lab} H_h - BIGPEN_{h,s,g}\, S_h - C^{fix}_h \tag{9}$$

Where π_{hki} (USD ha^{-1}) is the gross margin defined as $\pi_{hki} = p_{hki}\,\widehat{Y}_{hki} - c^{var}_{hki}$, with p_{hki} (USD t^{-1}) the output price, $\widehat{Y}_{hki}$ (t ha^{-1}) the surrogate-predicted yield coefficient, and c^{var}_{hki} (USD ha^{-1}) non-water variable production costs. Irrigation costs are represented by C^{water}_{hki} (USD ha^{-1}). Collective-intelligence priorities enter as an additive per-hectare social premium $\mu^{eff}_{s,g} w_{s,k,g}$ (USD ha^{-1}), where $w_{s,k,g}$ is the SSP- and layer-specific crop preference weight (dimensionless; $\sum_k w_{s,k,g} = 1$) and $\mu^{eff}_{s,g}$ scales the strength of the social incentive;

A_{hki} (ha) is the area allocated by household h to crop k under feasible management option $i \in I_h(k)$, and H_h (labor-days per cycle) is hired labor valued at wage rate w^{lab} (USD labor-day^{-1}). Deviations from the social-alignment rule are captured by the non-negative slack S_h (ha) and penalized by $BIGPEN_{h,s,g}$ (USD ha^{-1}) so that violations occur only when strict compliance is infeasible. Finally, C^{fix}_h (USD per cycle) denotes household fixed costs.

We compute the effective social-reward intensity as:

$$\mu^{\text{eff}}_{s,g} = \mu_{s,g} \cdot \text{scale}_h, \tag{10}$$

where $\mu_{s,g}$ is scenario-specific (Table S3) and $scale_h$ rescales the normative premium to the household's economic magnitude (see Appendix 2). Eq. (10) improves comparability across heterogeneous households.

Standard constraints. The household plan is bounded by land, water,

Table 4
Notation and core components of the household hydro-economic LP.

Block	Symbol	Description	Units
Indices/Sets	h, s, g	Household; SSP scenario; social-weight configuration (layer)	–
	$k \in K$	Crop index; $K = \{\text{maize, rice, beans, cassava}\}$	–
	$i \in I_h(k)$	Feasible management/ irrigation options for crop k at household h	–
Decision variables	A_{hki}	Area allocated to option (k,i)	ha
	H_h	Hired labor per cycle	labor-days cycle^{-1}
	$S_{h,s,g}$	Slack relaxing the minimum social-alignment constraint	ha
Biophysical (AquaCrop–AI)	$\widehat{Y}_{hki}$	Predicted yield	t ha^{-1}
	GIR_{hki}	Gross irrigation requirement	mm cycle^{-1}
Economic coefficients	p_{hki}	Output price	USD t^{-1}
	c^{var}_{hki}	Variable cost (excluding irrigation cost)	USD ha^{-1} cycle^{-1}
	C^{water}_{hki}	Irrigation cost per ha (Eq. (7))	USD ha^{-1} cycle^{-1}
Endowments/ Scarcity	A^{max}_h	Land endowment	ha
	$L^{max}_{h,s}$	Family labor endowment	labor-days cycle^{-1}
	B^{max}_h	Working capital (budget)	USD cycle^{-1}
	$W^{acc}_{h,s}$	Household-accessible water (Eq. (5))	mm·ha cycle^{-1}
Social alignment	$w_{s,k,g}$	SSP-specific crop preference weights (Eq. (3))	–
	$M_{s,g}$, $\alpha_{s,g}$	Top-M crop set; minimum alignment share (Eq. (15))	–
	$\mu^{eff}_{h,s,g}$	Effective social-reward intensity (Eq. (10))	USD ha^{-1}
	$BIGPEN_{h,s,g}$	Penalty on slack $S_{h,s,g}$ in the objective (Eq. (9))	USD ha^{-1}

Note. Monetary values are expressed in USD per cropping cycle. Water accounting uses 1 mm × 1 ha = 10 m^3 (Eq. (4)). The LP is solved independently for each (h,s,g).

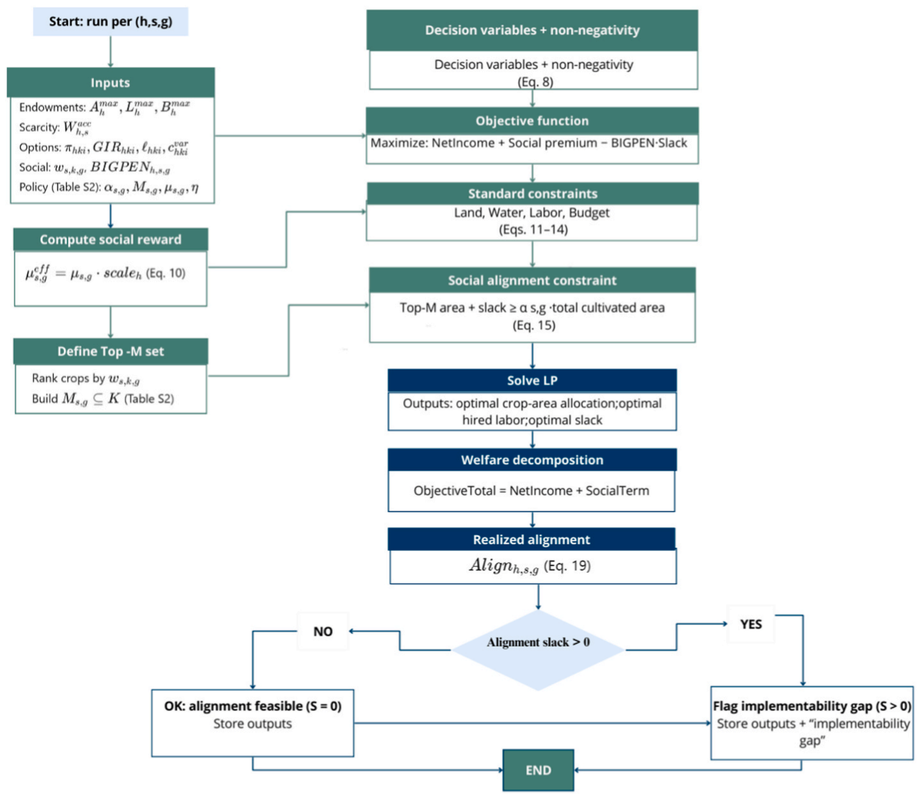

Fig. 3. Workflow for solving the household hydro-economic LP under SSP-specific social weights.

labor, and liquidity.

Land availability

$$\sum_{k\,\epsilon\,K}\sum_{i\,\epsilon\,I_h(k)} A_{hki} \le A_h^{max} \tag{11}$$

Eq. (11) limits total cultivated area by household land endowment.

Water availability

$$\sum_{k\,\epsilon\,K}\sum_{i\,\epsilon\,I_h(k)} GIR_{hki}\, A_{hki} \le W_{h,s}^{acc} \tag{12}$$

where GIR_{hki} is the gross irrigation requirement (mm·ha) and $W_{h,s}^{acc}$ is accessible seasonal irrigation water under SSP s. Eq. (12) enforces hydrologic scarcity.

Labor feasibility

$$\sum_{k\,\epsilon\,K}\sum_{i\,\epsilon\,I_h(k)} \ell_{hki}\, A_{hki} \le L_h^{max} + H_h \tag{13}$$

where ℓ_{hki} is labor demand (days ha^{-1}) and L_h^{max} is available family labor. Eq. (13) allows hired labor H_h to relax the labor constraint at a cost in Eq. (9).

Budget feasibility

$$\sum_{k\,\epsilon\,K}\sum_{i\,\epsilon\,I_h(k)} c_{hki}^{var} A_{hki} \le B_h^{max} \tag{14}$$

Eq. (14) prevents unrealistically capital-intensive plans by enforcing seasonal liquidity limits.

2.5.3. *Social alignment mechanism: Top-**M** set, minimum share, and feasibility safeguard*

Section 2.4 produces SSP-conditional crop preference weights $w_{s,k,g}$ for each social layer $g \in \{\text{Low}, \text{Base}, \text{High}, \text{Uniform}, \text{Favored}\}$. In the LP, these weights are operationalized through (i) a continuous incentive in the objective (Eq. (9)) and (ii) a minimum alignment share enforced through a linear constraint with a penalized slack.

Top-M priority set. For each (s,g), crops are ranked by the posterior preference weight $w_{s,k,g}$ in descending order. The priority set $M_{s,g} \subseteq K$ is then defined as the M highest-ranked crops, where M is SSP-specific (Table S3). This mapping turns the continuous preference vector into an explicit subset used by the alignment rule.

Minimum alignment share with penalized slack. We require that at least a fraction $\alpha_{s,g}$ of each household's cultivated area is allocated to crops in $M_{s,g}$:

$$\sum_{k\,\epsilon\,M_{s,g}}\sum_{i\,\epsilon\,I_h(k)} A_{hki} + S_h \ge \alpha_{s,g} \sum_{k\,\epsilon\,K}\sum_{i\,\epsilon\,I_h(k)} A_{hki},\; S_{h,s,g} \ge 0 \tag{15}$$

Equation (15) enforces adherence to collective priorities while preserving feasibility when land, water, labor, budget, or diversification constraints bind. The slack variable $S_{h,s,g}$ (ha) quantifies the alignment shortfall relative to the target share and is penalized in the objective function (Eq. (9)) through $BIGPEN_{h,s,g}$. Consequently, $S_{h,s,g} > 0$ indicates that the requested alignment is not fully attainable under binding constraints, rather than a costless relaxation.

Operationally,

$$S_{h,s,g} = \max\left(0, \alpha_{s,g} A_h^{tot} - A_{h,s,g}^{M}\right),$$

where $A_h^{tot} = \sum_{k\in K}\sum_{i\in I_h(k)} A_{hki}$ is total cultivated area; $A_{h,s,g}^{M} = \sum_{k\in M_{s,g}}\sum_{i\in I_h(k)} A_{hki}$ is the area allocated to the Top-M set. The penalty is set sufficiently large so that slack is activated only as a last resort to maintain feasibility, thereby minimizing deviations from the alignment target.

To avoid over-penalization in low-margin households and improve numerical stability, we scale the penalty to within-household profit magnitudes:

$BIGPEN_{h,s,g} = c \times q_{0.95}\,(\pi_{hki})$, where $q_{0.95}(\pi_{hki})$ is the within-household 95th percentile of option gross margins (Eq. (8)), and c is a fixed multiplier applied uniformly across (s, g). The implications of this scaling for slack activation and the alignment–income trade-off under tightened (M, α) targets are documented in Appendix 3 (SSP3 stress-test; Table A3.1 and Figures A3.1–A3.2).

2.5.4. Scenario design, solution procedure, and reported outputs

We solve the LP defined by Eqs. (8)–(15) for each combination of household h, SSP s, and social-weight layer g. This produces a fully factorial set of runs that supports both aggregate and distributional analysis of economic–social trade-offs and the feasibility of normative steering under binding constraints.

Solution procedure and feasibility. Because the objective (Eq. (9)) and constraints (Eqs. (11)–(14)) are linear, each instance is solved to optimality with a standard LP solver. Feasibility is preserved by construction through the slack S_h in Eq. (15); when $S_h > 0$, solutions remain comparable across scenarios while transparently recording deviations from alignment targets.

Primary outputs. For each (h, s, g), we store: (i) optimal land allocation A^*_{hki} and implied crop shares; (ii) slack S^*_h; and (iii) decomposed welfare components consistent with Eq. (15):

$$Net\ Income_{h,s,g} = \sum_{k\ \epsilon\ Ki}\ \sum_{\epsilon\ I_h(k)} \left(\pi_{hki} - C^{water}_{hki}\right) A^*_{hki} - w^{lab} H^*_h - c^{fix}_h \tag{16}$$

$$Social\ term_{\ h,s,g} = \sum_{k\ \epsilon\ Ki}\ \sum_{\epsilon\ I_h(k)} \left(\mu^{eff}_{s,g}\ w_{s,k,g}\right) A^*_{hki} - BIGPEN_{h,s,g} S^*_h \tag{17}$$

$$Objective\ total_{h,s,g} = Net\ Income_{h,s,g} + Social\ term_{\ h,s,g} \tag{18}$$

Eqs. (16)–(18) provide a transparent decomposition of the optimization outcome into private and normative components, enabling interpretable comparisons across SSPs, social layers, and household vulnerability strata.

Optionally, we report the realized alignment share implied by Eq. (19):

$$\mathrm{align}_{h,s,g} = \frac{\sum\limits_{k \in M_{s,g}} \sum\limits_{i \in I_h(k)} A^*_{hki}}{\sum\limits_{k \in Ki} \sum\limits_{i \in I_h(k)} A^*_{hki}} \tag{19}$$

Eq. (19) summarizes adherence to the prioritized crop set, while S^*_h identifies cases where the alignment target is not implementable under binding constraints.

For reproducibility, Appendix 4 provides a worked numerical example that walks through a single (h, s, g) run step-by-step, showing how inputs are transformed into LP coefficients, constraints, and reported outputs.

2.5.5. Diversification (3-of-4) via LP-preserving enumeration

To enforce a minimum of three cultivated crops without introducing mixed-integer complexity, diversification is implemented by solving four LPs for each (h, s, g), each excluding one crop $k \in K$ and imposing a minimum area constraint on the remaining crops. The minimum area threshold is:

$$A^{min}_h = \min\left\{A^{cap}, \max\left(A^{fix}, \rho A^{max}_h\right)\right\}, A^{min}_h \leq 0.95\left(\frac{A^{max}_h}{3}\right) \tag{20}$$

with $A^{cap} = 0.25$ ha, $A^{fix} = 0.10$ ha, and $\rho = 0.02$. Among the four candidate solutions, the feasible solution maximizing Eq. (9) is retained as the household outcome under (s, g). An optional feasibility filter requiring net income ≥ 0 was available but not applied in the main specification.

2.6. Economic coefficients and SSP mapping under a drought (dry-year Typical Meteorological Year) setting

This section documents the economic coefficients and household resources used in the hydro-economic LP and clarifies the SSP mapping adopted in this study. For each household h, crop $k \in K$, and management option $i \in I_h(k)$, we define the private (non-water) gross margin π_{hki} (USD ha^{-1} cycle^{-1}), variable production cost c^{var}_{hki} (USD ha^{-1} cycle^{-1}), and labor requirement l_{hki} (labor-days ha^{-1} cycle^{-1}). Baseline crop budgets and unit values used to construct these parameters are reported in Table S5.

Household endowments are taken directly from the survey dataset (Section 2.1): land availability A^{max}_h (ha), family labor L^{max}_h (labor-days per cycle), and seasonal liquidity B^{max}_h (USD per cycle). Hired labor $H_{h,i}$ is allowed at a constant wage w^{lab} (USD labor-day^{-1}), and fixed household costs c^{fix}_h (USD cycle^{-1}) enter as a lump-sum term. Crop sale prices and unit production budgets—and therefore π_{hki} and c^{var}_{hki}—are held constant across SSPs.

Biophysical inputs vary across households but are computed under a representative drought (dry-year TMY) climate used to generate predicted yield $\hat{y}_{h,k}$ and gross irrigation depth $GIR_{h,k}$. Conditional on this drought setting, we hold $\hat{y}_{h,k}$ and $GIR_{h,k}$ constant across SSPs for each household–crop pair, i.e., $\hat{y}_{h,k,s} = \hat{y}_{h,k}$ and $GIR_{h,k,s} = GIR_{h,k}$ for all s. Under this ceteris paribus mapping, the only SSP-varying inputs entering the LP are the SSP-specific crop preference weights $w_{s,k}$ inferred in Section 2.4 (and any derived Top-M sets or social-weight layers). Consequently, cross-SSP differences in allocations and welfare isolate the effect of alternative collective priorities evaluated on a common drought-stress feasibility space, rather than reflecting changes in markets, household endowments, or agronomic requirements.

2.7. Model implementation, outputs, and diagnostics

The workflow was implemented in R 4.5.0 (lpSolve) and executed for each household across all SSPs and weight configurations. Outputs were stored as: (i) household × SSP × configuration summaries (crop areas, water use, net income, social reward contribution, alignment share, slack activation), and (ii) option-level audit tables to enable coefficient traceability.

3. Results

3.1. Biophysical module results: AquaCrop surrogates and household coefficients

Household-level biophysical inputs to hydro-economic optimization show clear cross-crop contrasts and meaningful within-crop heterogeneity under the dry-year baseline. Fig. 4 summarizes the distributions of surrogate-derived yield coefficients $\hat{Y}$ (t ha^{-1}) and gross irrigation depth GIR (mm cycle^{-1}) used to parameterize the household LP. Yield dispersion is highest for maize (median 5.32 t ha^{-1}; IQR 0.62) and rice (median 4.88; IQR 0.34), whereas beans and cassava exhibit much tighter yield distributions (IQR $\approx$ 0.11 for both). These patterns indicate that, in the drought benchmark, spatial variation in productive potential is more pronounced for cereals than for beans and cassava across surveyed households.

Irrigation requirements display stronger asymmetry and wider tails than yields, reflecting both crop-specific water demand and heterogeneity in household-local growing conditions. Beans require the lowest irrigation depth on average (median GIR 63 mm cycle^{-1}), followed by maize (180 mm cycle^{-1}), while rice (320 mm cycle^{-1}) and cassava (252 mm cycle^{-1}) exhibit substantially higher irrigation intensity (Fig. 4B; Table 5). The wide P5–P95 ranges—especially for rice and cassava—highlight that a non-trivial subset of households faces markedly higher irrigation needs even within the same crop, a feature that is propagated into the feasibility and cost constraints of the optimization. Consistent with the modeling framework, the surrogate emulates net irrigation requirements (NIR), which are converted to applied irrigation

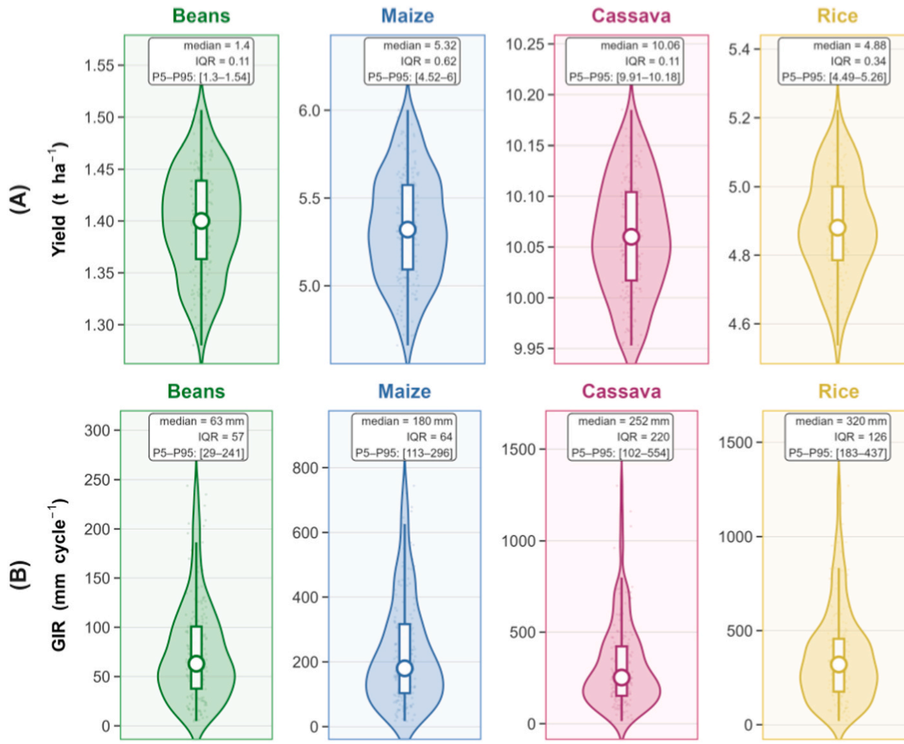

Fig. 4. Biophysical module outputs used in the LP. A. Distributions of predicted yield coefficients $\widehat{Y}$; B. Gross irrigation depth *GIR* by crop (dry-year baseline; $n = 168$ households per crop).

Table 5
Summary of surrogate-derived household biophysical coefficients under the dry-year baseline (n = 168 households per crop).

Crop	N	$\widehat{Y}$ median (t ha^{-1})	$\widehat{Y}$ IQR (t ha^{-1})	$\widehat{Y}$ P5–P95 (t ha^{-1})	GIR median (mm cycle^{-1})	GIR IQR (mm cycle^{-1})	GIR P5–P95 (mm cycle^{-1})
Maize	168	5.32	0.62	4.52–6.00	180	64	113–296
Rice	168	4.88	0.34	4.49–5.26	320	126	183–437
Beans	168	1.40	0.11	1.30–1.54	63	57	29–241
Cassava	168	10.06	0.11	9.91–10.18	252	220	102-554

depth using a fixed irrigation efficiency, $GIR = NIR/\eta$, with $\eta = 0.60$ for water accounting consistency across modules.

Surrogate validity is supported by crop-specific observed–predicted diagnostics evaluated on held-out AquaCrop simulations, where "observed" denotes AquaCrop-simulated outcomes and "predicted" denotes XGBoost outputs for the same test cases. Figs. 5 and 6 show tight clustering around the 1:1 line across crops, with fitted trends closely tracking proportionality and limited systematic bias. These diagnostics are consistent with the reported test-set skill (yield $R^2 = 0.89$–0.93; NIR $R^2 = 0.87$–0.91; Methods), indicating that the surrogate reproduces the AquaCrop response surface with sufficient fidelity for coefficient generation. Finally, optimization-relevant perturbation checks confirm that the main allocation patterns are structurally driven by feasibility constraints and preference scenarios rather than minor surrogate noise: re-solving the LP under $\pm10\%$ shocks to $\widehat{Y}$ and $\widehat{NIR}$ did not materially change dominant crop choices or key allocation shares.

3.2. Collective intelligence outputs: SSP strategy lenses and Bayesian crop-preference posteriors

Collective priorities varied systematically across SSP narratives and mirrored the dominant stakeholder strategy lenses. Under SSP1, which emphasizes climate-resilient food production and irrigation efficiency, posterior mass concentrates on beans and maize, while rice is comparatively down-weighted, consistent with water-efficiency considerations. Under SSP3, characterized by decentralized rainwater harvesting and limited institutional support, preferences shift toward cassava and beans, and rice is consistently ranked last. In contrast, SSP4, anchored in fair market access and cooperative marketing, yields a more market-oriented profile that prioritizes maize and rice.

Bayesian aggregation produces SSP-specific crop-preference weights $w_{s,k}$ as probabilistic inputs to the optimization model (Table 6; Fig. 7). In SSP1, beans has the highest posterior mean (0.305 [0.259–0.352]), followed by maize (0.243 [0.200–0.288]), with cassava (0.228 [0.187–0.272]) and rice (0.224 [0.183–0.268]) slightly lower. In SSP3, cassava ranks first (0.323 [0.277–0.372]) and beans second (0.276 [0.232–0.323]), while rice remains lowest (0.173 [0.136–0.214]). In SSP4, maize ranks first (0.302 [0.257–0.350]) and rice second (0.262 [0.219–0.308]), followed by beans and cassava.

To distinguish uncertainty in magnitude from uncertainty in ordering, we interpret "consensus" as posterior rank stability rather than dispersion of $w_{s,k}$. For each SSP, we draw samples from the Dirichlet posterior and compute $p_{\text{top2}} = \Pr\left(\text{rank}_{s,k} \leq 2\right)$, the probability that crop k appears among the Top-2 priorities across posterior draws. High p_{top2} indicates robust prioritization despite posterior uncertainty, whereas low values indicate rank instability and competition among alternatives. In SSP1, beans shows near-certain Top-2 membership ($p_{\text{top2}} = 0.99$), while the remaining crops exhibit substantially lower Top-2 probabilities, reflecting contestation for the second position. A similar pattern holds in SSP3 and SSP4, where the leading crops (cassava in SSP3; maize in SSP4) are highly stable, whereas lower-ranked crops display weaker

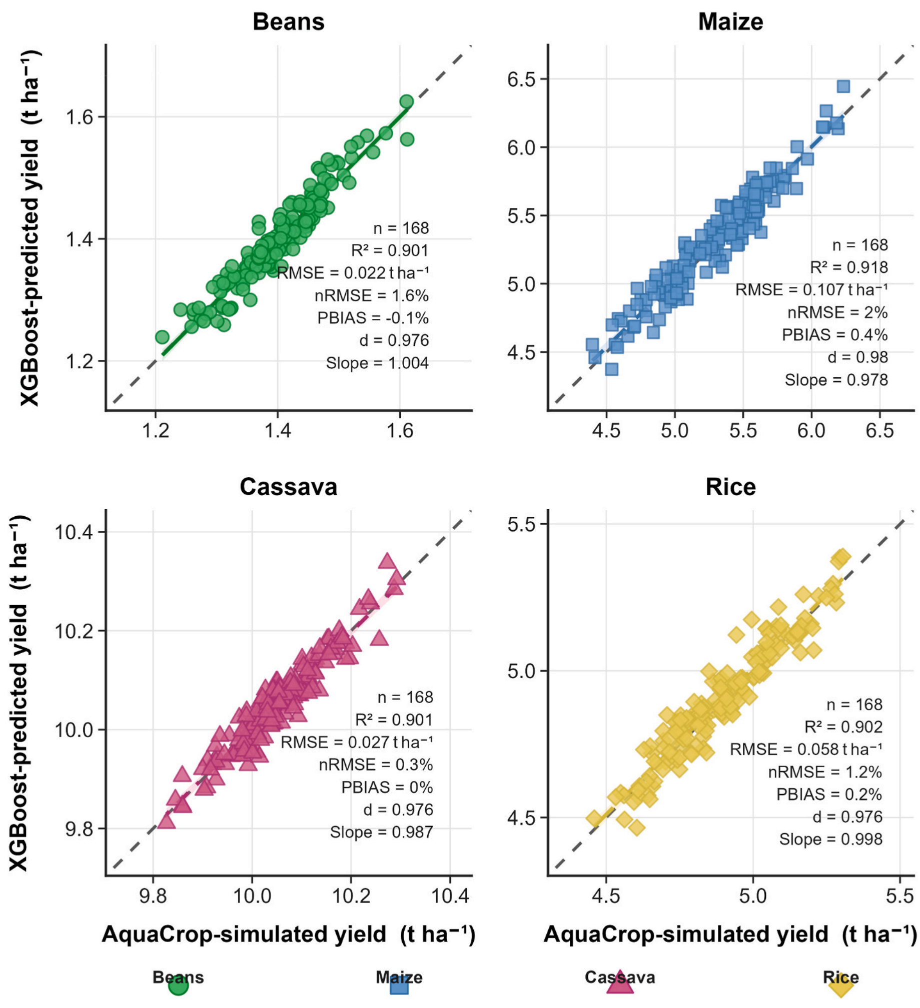

Fig. 5. Surrogate diagnostics for yield: observed (AquaCrop) vs predicted (XGBoost) by crop (test split).

rank stability (Table 6). Accordingly, credible-interval widths summarize uncertainty in weight magnitude, while p_{top2} captures uncertainty in ordering—the property that directly informs downstream Top-M alignment and diversification constraints.

While Table 6 summarizes posterior crop-preference weights and their rank stability, the hydro-economic LP requires layer-specific prioritization inputs. Table S6 therefore reports the associated rankings and the induced Top-M sets $M_{s,g}$ used by the alignment constraint. Across SSPs, the leading crops remain unchanged across Base/Low/High (beans in SSP1, cassava in SSP3, maize in SSP4), indicating that the identity of the dominant priorities is robust to posterior uncertainty. Variation arises mainly in the breadth of prioritization: Low typically yields a more conservative Top-M ($M_{s,g} = 2$), whereas Base/High generally retain $M_{s,g} = 3$. The Uniform benchmark expands prioritization to all crops ($M_{s,g} = 4$), and the Favored stress test introduces SSP-consistent tilts in the prioritized set (e.g., SSP1 shifts the lead to rice). Together, these layer-dependent $M_{s,g}$ configurations provide the channel through which preference uncertainty and normative prioritization enter the LP and propagate into the hydro-economic solutions.

3.3. *Hydro-economic outcomes: feasibility, welfare composition, and scarcity signals*

The framework produced 2520 household–scenario solutions (168 households × 3 SSPs × 5 social-weight layers $g \in G$), achieving full coverage of all (h, s, g) combinations (Table 7). The diversification wrapper is binding by construction, yielding exactly three cultivated crops per solution. Importantly, the alignment constraint remained feasible throughout: the penalized alignment slack was never activated ($S_{h,s,g} = 0$ in 100% of runs), indicating that the baseline $\alpha_{s,g}$ and $M_{s,g}$ targets lie within households' feasible allocation sets under the assumed scarcity constraints. To verify that slack behaves as intended when alignment targets become non-implementable, we conduct a targeted SSP3/Base stress-test that tightens the Top-M set ($M \in \{2, 1\}$) and increases α up to 0.99; slack remains zero for moderate targets but rises sharply only under extreme requirements, revealing an alignment–income trade-off near the infeasibility region (Appendix 3; Fig. A3.1; Table A3.2).

Objective decomposition isolates the welfare mechanism induced by the social layer. Across SSP, increasing normative leverage (i.e., moving from Low/Base toward High/Favored) systematically raises the Social term, while Net income remains largely stable in SSP1 and SSP4 (Fig. 8; Table 7). In SSP4, the mean objective increases from USD 8334.0 (Base) to USD 11,426.9 (Favored), driven almost entirely by the Social term (USD 3282.6 → 6382.4) with negligible variation in Net income (USD 5051.4 → 5044.5). SSP1 follows the same pattern at smaller magnitude: Base-to-Favored increases the objective from USD 7290.9 to USD 8405.8, mainly via the Social term (USD 2224.2 → 3386.0) with only a modest reduction in Net income (USD 5066.7 → 5019.8) (Table 7). These results indicate high compatibility between collectively elicited priorities and the private feasibility frontier in SSP1 and SSP4. Here, 'normative leverage' reflects the combined effect of (i) the chosen social-

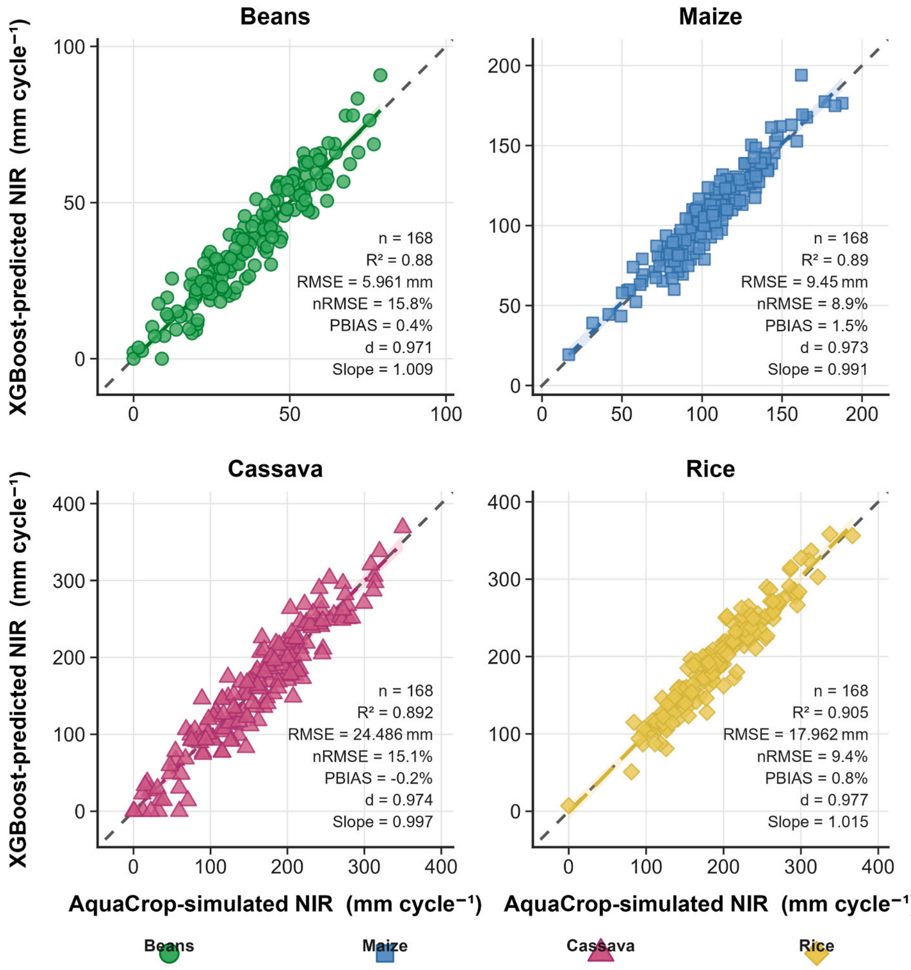

Fig. 6. Surrogate diagnostics for NIR: observed (AquaCrop) vs predicted (XGBoost) by crop (test split).

Table 6
SSP-specific Bayesian posterior crop-preference weights and rank-stability diagnostics (Top-2 probability).

SSP	Crop	w (s,k) [95% CrI]	Rank	CI width	Consensus	Robustness
SSP1	Beans	0.305 [0.259–0.352]	1	0.093	High Consensus	0.99 (Very High)
SSP1	Maize	0.243 [0.200–0.288]	2	0.087	High Controversy	0.53 (Low)
SSP1	Cassava	0.228 [0.187–0.272]	3	0.085	High Controversy	0.26 (Low)
SSP1	Rice	0.224 [0.183–0.268]	4	0.085	High Controversy	0.21 (Low)
SSP3	Cassava	0.323 [0.277–0.372]	1	0.096	High Consensus	1.00 (Very High)
SSP3	Beans	0.276 [0.232–0.323]	2	0.091	High Consensus	0.91 (High)
SSP3	Maize	0.227 [0.186–0.271]	3	0.085	High Controversy	0.09 (Low)
SSP3	Rice	0.173 [0.136–0.214]	4	0.078	High Controversy	0.00 (Low)
SSP4	Maize	0.302 [0.257–0.350]	1	0.093	High Consensus	0.98 (Very High)
SSP4	Rice	0.262 [0.219–0.308]	2	0.089	Moderate Consensus	0.76 (Moderate)
SSP4	Beans	0.236 [0.194–0.281]	3	0.087	High Controversy	0.24 (Low)
SSP4	Cassava	0.200 [0.160–0.242]	4	0.082	High Controversy	0.02 (Low)

Note: $w_{s,k}$ is the SSP-specific posterior crop-preference weight (posterior mean and 95% CrI). CrI width $= CI_{0.975} - CI_{0.025}$. Robustness is the Top-2 probability $p_{\text{top2}} = \Pr\left(\text{rank}_{s,k} \le 2\right)$, estimated from Dirichlet posterior draws by ranking crops within each draw. Consensus is a stability tier based on p_{top2}: High Consensus (≥ 0.80), Moderate Consensus (0.60–$<$ 0.80), High Controversy ($<$ 0.60). This indicates Top-2 rank stability (relevant for Top-*M* alignment), not a psychometric agreement metric.

weight layer (which changes the relative priority vector across crops) and (ii) the SSP × configuration implementation parameters (αs,g, μs,g) that translate priorities into binding incentives/requirements.

In contrast, SSP3 reveals a scarcity-sensitive trade-off between normative steering and private welfare. Under SSP3–Low, alignment falls sharply (Share $\left(M_{s,g}\right) = 0.582$) and Net income declines to USD 3660.8, coinciding with higher scarcity signals (Water utilization 0.582; Binding rate 22.02%). Under SSP3–Favored, the objective increases to USD 7481.8 through a larger Social term (USD 2901.7), but Net income remains below Base (USD 4580.1 vs 5069.0), consistent with a normative–feasibility tension when water constraints bind more frequently (Table 7).

A structural allocation outcome underlying these patterns is the near-systematic exclusion of rice under baseline biophysical–economic

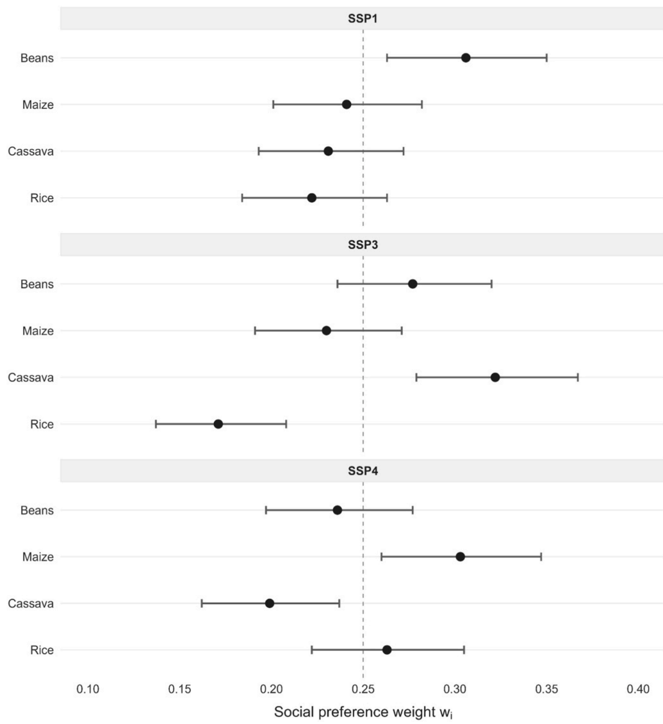

Fig. 7. Bayesian posterior means with 95% credible intervals for $w_{s,k}$ by SSP.

coefficients. The rice-exclusion diagnostic (Fig. S1) shows that exclusion weakens under stronger normative leverage; for example, in SSP1–Favored, rice remains excluded by ~59% of households. This indicates that the collective-intelligence layer can reconfigure cropping portfolios when normative incentives are sufficiently strong to offset baseline comparative disadvantage (Table 7).

3.4. Mechanism test: how α_s and μ_s shift welfare composition and reveal normative–feasibility tension

Results support the proposed mechanism: increasing normative leverage—implemented through higher minimum alignment requirements ($\alpha_{s,g}$) and stronger monetization of the social reward ($\mu_{s,g}$)—raises the social term systematically, with limited disruption of Net income enabling futures. In SSP4, mean objective value increases from USD 8334 (Base) to USD 11,427 (Favored), almost entirely driven by the social term (USD 3283 → 6382) while Net income remains stable (USD 5051 → 5045; Table 7). SSP1 exhibits the same pattern at smaller magnitude (objective USD 7291 → 8406; Social term USD 2224 → 3386; Net income USD 5067 → 5020), indicating high compatibility between collective priorities and the feasible income frontier in SSP1 and SSP4 (Table 7).

SSP3 provides the stress-test contrast where feasibility constraints become binding more often and normative steering is no longer "low-regret." Under SSP3–Low, alignment with the preferred set decreases sharply (share $M_{s,g} = 0.582$) and Net income drops to USD 3,661, concurrent with higher scarcity signals (water utilization = 0.582; binding rate = 22.0%; Table 7). Under SSP3–Favored, the objective increases to USD 7482 due to a larger social term (USD 2902), but Net income remains below Base (USD 4580 vs 5069), evidencing a normative–feasibility tension: strengthening preference-consistent allocation becomes welfare-costly when water constraints bind more frequently and the preferred crops intensify scarcity pressure (Table 7).

Overall, the SSP4–SSP3 contrast is policy-relevant because it delineates when preference-consistent targeting is compatible with feasibility (SSP1/SSP4) versus when it requires complementary investments (e.g., improved water access, irrigation efficiency, or enabling institutions) to avoid private welfare losses under constrained futures (SSP3).

3.5. Distributional outcomes: vulnerability (SEVI) gradients reflect capability constraints, not preference exclusion

Distribution patterns were assessed across terciles of the Socioeconomic Vulnerability Index (SEVI), a household-level indicator computed for each surveyed household by Polo-Murcia et al. (2026). We stratify households by SEVI terciles (T1: least vulnerable; T3: most vulnerable) and compare mean net income across the five social-weight layers (Low, Base, High, Uniform, Favored). Distributional outcomes under social-weight layers across vulnerability terciles. Table 8 summarizes how the total LP objective (net income plus the social term) is distributed across SEVI terciles under each social-weight layer and SSP. Across all scenarios, the objective exhibits a clear vulnerability gradient, with

Table 7
Mean LP outcomes by SSP and social-weight regime.

Social-weight layers	Net income mean (USD)	Social term mean (USD)	Objective mean (USD)	Share (*align*$_{h,s,g}$)	Water util. mean	Binding rate (%)
SSP1						
Low	5056.50	1547.60	6604.20	0.958	0.535	12.5
Base	5066.70	2224.20	7290.90	1	0.532	12.5
High	5066.50	2897.90	7964.40	1	0.532	12.5
Uniform	5069.60	1832.80	6902.40	1	0.532	12.5
Favored	5019.80	3386.00	8405.80	0.97	0.535	11.31
SSP3						
Low	3660.80	1303.20	4964.00	0.582	0.582	22.02
Base	5069.00	1747.70	6816.70	1	0.526	12.5
High	5069.00	2285.10	7354.10	1	0.526	12.5
Uniform	5069.60	1466.30	6535.80	1	0.532	12.5
Favored	4580.10	2901.70	7481.80	1	0.59	22.02
SSP4						
Low	5051.50	2342.90	7394.30	0.936	0.536	12.5
Base	5051.40	3282.60	8334.00	0.966	0.536	12.5
High	5049.30	4203.30	9252.60	0.968	0.537	12.5
Uniform	5067.60	2201.60	7269.30	1	0.532	12.5
Favored	5044.50	6382.40	11,426.90	0.97	0.537	12.5

Note: n = 168 households per row. Share $\left(\text{align}_{h,s,g}\right)$ is the realized cultivated-area share allocated to the SSP-specific Top-M priority set. Water util. is mean irrigation-water utilization (water used/water available). Binding rate (%) is the share of households with a binding water constraint (water used = water available). In the main specification, the alignment rule is implementable for all (h,s,g), so $S_{h,s,g} = 0$ in 100% of solutions; implementability thresholds under tightened (M, α) are reported in Appendix 3 (Fig. A3.1; Table A3.2).

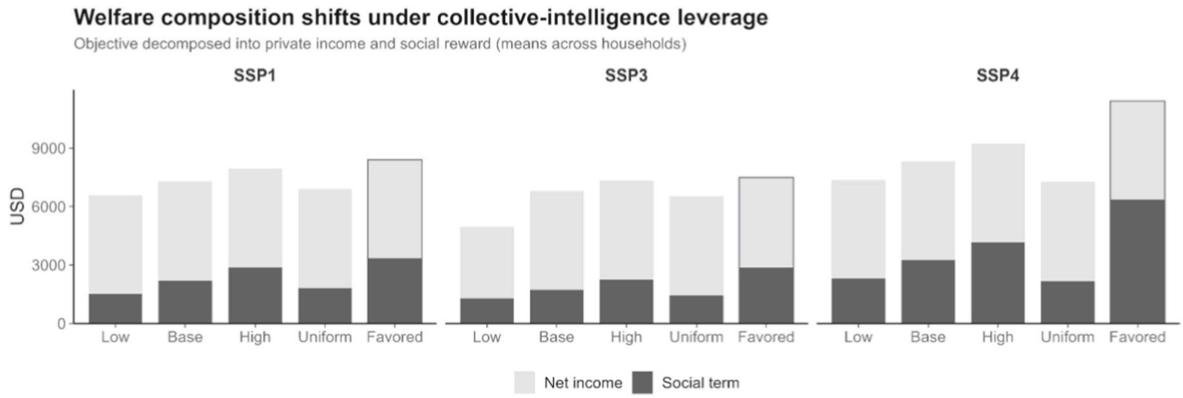

Fig. 8. Objective decomposition into Net income and Social term across social-weight layers by SSP.

Table 8
Distributional outcomes of the LP objective across SEVI terciles under alternative social-weight layers (median [IQR], USD cycle^{-1}), by SSP.

SSP	Layer	T1 Total objective (median [IQR])	T2 Total objective (median [IQR])	T3 Total objective (median [IQR])	Δ(T1−T3) objective (USD)	Median social share (social/objective)
SSP1	Low	8029 [6277–10,163]	6129 [5168–7700]	4837 [3813–5957]	3192	0.252
SSP1	Base	8850 [7046–11,046]	6838 [5735–8421]	5447 [4306–6561]	3403	0.322
SSP1	High	9634 [7736–11,876]	7547 [6321–9164]	6052 [4828–7155]	3582	0.383
SSP1	Uniform	8381 [6600–10,542]	6430 [5408–8011]	5095 [4013–6212]	3286	0.283
SSP1	Favored	10,227 [8243–12,381]	8028 [6729–9718]	6435 [5166–7496]	3793	0.427
SSP3	Low	5918 [5246–7103]	4906 [4144–5636]	3877 [3063–4464]	2041	0.268
SSP3	Base	8231 [6663–10,382]	6334 [5315–7882]	4991 [3931–6112]	3240	0.272
SSP3	High	8877 [7198–11,076]	6923 [5760–8449]	5471 [4329–6588]	3405	0.329
SSP3	Uniform	7937 [6192–10,062]	6047 [5091–7623]	4765 [3760–5885]	3171	0.240
SSP3	Favored	9338 [8014–10,457]	7490 [6072–8655]	5777 [4526–6420]	3562	0.523
SSP4	Low	9002 [7191–11,200]	6960 [5820–8547]	5546 [4380–6646]	3456	0.337
SSP4	Base	10,130 [8135–12,325]	7940 [6660–9621]	6381 [5121–7454]	3749	0.416
SSP4	High	11,243 [9181–13,388]	8899 [7516–10,680]	7185 [5830–8235]	4058	0.477
SSP4	Uniform	8825 [7022–11,019]	6814 [5713–8400]	5425 [4285–6537]	3400	0.322
SSP4	Favored	13,644 [11,453–15,776]	11,185 [9533–13,153]	9029 [7267–10,015]	4614	0.580

Notes: The LP objective equals Total objective = Net income + Social term. T1 = least vulnerable; T3 = most vulnerable. IQR = interquartile range (25th–75th percentiles). Δ(T1−T3) is computed from tercile medians. Each tercile contains N = 56 households (total N = 168 per SSP × layer).

T1 (least vulnerable) consistently achieving higher objective values than T3 (most vulnerable). The resulting median gap Δ(T1−T3) remains sizeable in every SSP–layer combination, ranging from 2041 USD (SSP3–Low) to 4614 USD (SSP4–Favored). This persistence indicates that, even when normative targeting is operationalized within the optimization, structural constraints linked to vulnerability continue to shape feasible welfare outcomes, rather than being eliminated by preference reweighting alone.

Within each SSP, tightening the normative signal generally increases objective levels across terciles. In SSP1, moving from Low to Favored increases the median objective from 8029 to 10,227 USD in T1 and from 4837 to 6435 USD in T3, while the social share rises from 0.252 to 0.427, showing that improvements are partly driven by greater normative contribution in the objective. A similar pattern holds in SSP3, where the Low configuration yields the lowest median objective levels (T3: 3877 USD) and Favored produces the highest (T3: 5777 USD), accompanied by a marked rise in the median social share (0.268 → 0.523). In SSP4, the contrast is strongest: Favored raises the median objective to 13,644 USD (T1) and 9029 USD (T3), and the social share reaches 0.580, underscoring that the normative term becomes a major component of the optimized welfare metric under this configuration.

Importantly, while layers tend to lift objective levels, they do not systematically compress inequality. In fact, Δ(T1−T3) is often stable or increases slightly as the normative leverage intensifies (e.g., SSP1: 3192 → 3793 USD from Low to Favored; SSP4: 3456 → 4614 USD). This pattern is consistent with a setting where preference-consistent targeting is feasible and welfare-improving, yet the most vulnerable households remain more tightly constrained (e.g., by water, land, or labor) and therefore cannot translate the same marginal shifts in prioritization into proportional objective gains. Overall, Table 8 provides direct evidence that embedding SSP-conditional social weights in the objective function produces measurable and scenario-dependent changes in welfare, while simultaneously revealing that distributional disparities across vulnerability terciles persist under binding feasibility constraints.

In line with Table 8, Fig. 9 shows that net income distributions shift upward from Low/Uniform to High/Favored across SSPs, yet T3 households consistently remain below T1, indicating that vulnerability-driven constraints persist even when social-weight layers improve outcomes.

Across Socioeconomic Vulnerability Index (SEVI) terciles (T1–T3), optimized cultivated-area shares are highly stable in SSP1 and SSP4 across all social-weight layers (Low, Base, High, Uniform, Favored). As shown in Fig. 10 A (SSP1) and Fig. 10 C (SSP4), maize consistently dominates cultivated area, while beans, rice, and cassava remain marginal; even the Favored social-weight layer induces only minor second-order reallocations that do not change the portfolio hierarchy. In sharp contrast, Fig. 10B (SSP3) reveals clear sensitivity to both vulnerability and normative leverage: under the Favored social-weight layer, cultivated area shifts away from maize toward cassava, with the largest reallocations concentrated in T3 (most vulnerable). This pattern is consistent with a scenario-conditional normative–feasibility tension, whereby stronger collective-preference steering becomes allocation-relevant primarily when feasibility is tighter and capability constraints bind more strongly; nonetheless, rice remains consistently negligible across SEVI terciles and social-weight layers, reinforcing its weak baseline position under the prevailing water–return trade-off.

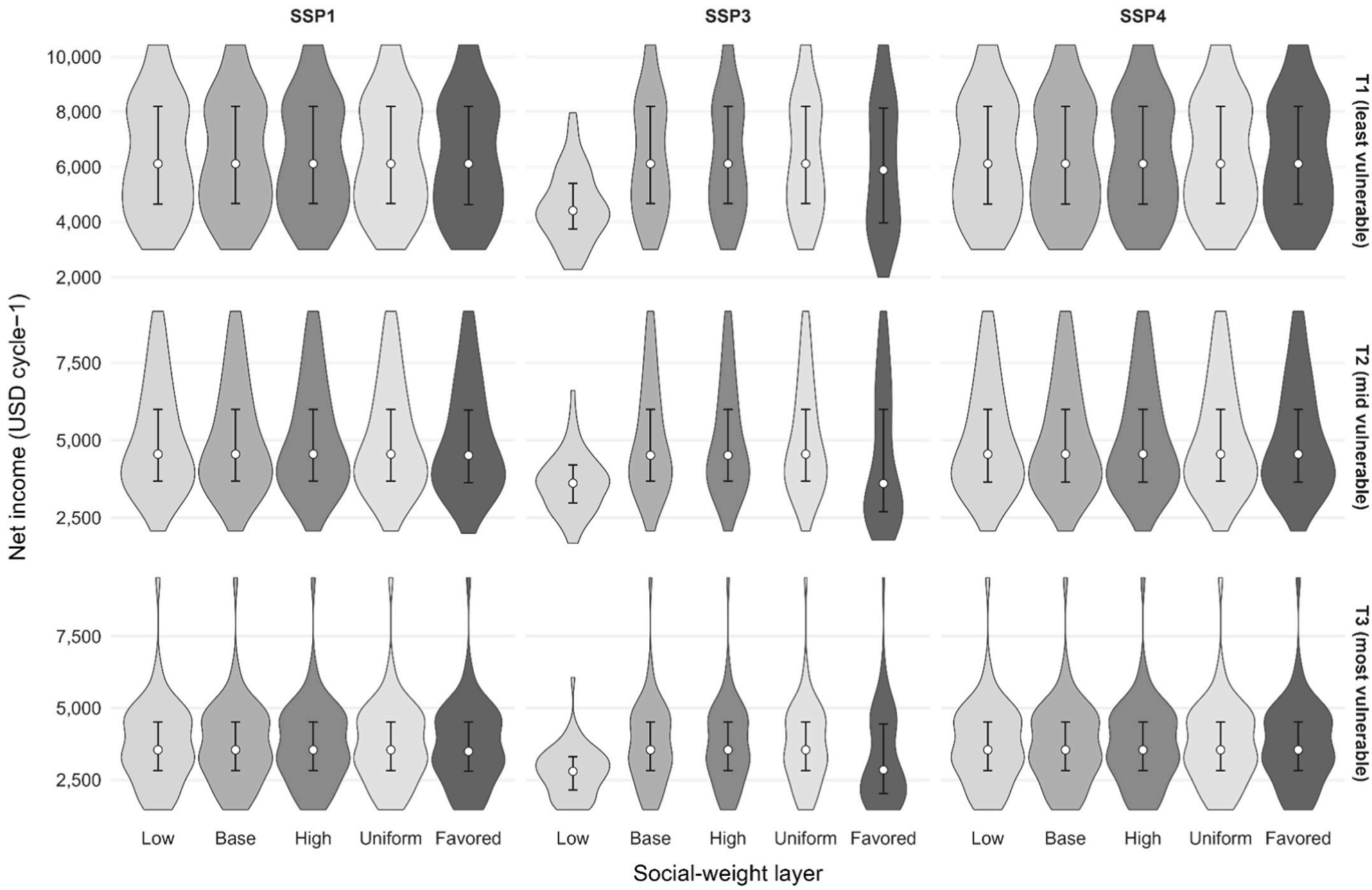

Fig. 9. Net income distributions across Socioeconomic Vulnerability Index (SEVI) terciles under the Base social-weight layer.

4. Discussion

This study advances irrigation decision support by operationalizing collective intelligence as an uncertainty-aware normative input and testing—rather than presuming—its implementability within a household-scale hydro-economic optimizer. Hydro-economic models are a mature class of tools for quantifying how binding constraints (water, land, labor) shape feasible allocations and welfare outcomes, yet stakeholder priorities are still commonly treated as qualitative guidance or fixed scenario assumptions rather than as probabilistic information that can be propagated through optimization and confronted with feasibility (Harou et al., 2009; Razavi et al., 2025). By embedding SSP-conditional posterior weights $w_{s,k}$ directly in the objective function and evaluating the induced allocations under explicit constraints, the framework makes preference-consistent targeting testable and auditably implementable—moving normative claims from deliberation to constraint-aware evaluation. Concretely, comparing normative layers (Base/Low/High/Uniform/Favored) within each SSP shows how alignment pressure and social-reward monetization reorder the optimal crop portfolio and allows us to assess whether greater social coherence is achieved with marginal private costs or with welfare losses—an empirical distinction that cannot be inferred from static rankings. This directly responds to a recurring direction in the HEM literature: the need to better integrate stakeholder perspectives and equity-relevant considerations beyond predominantly biophysical and economic indicators (Ortiz-Partida et al., 2023). As in many hydroeconomic case-study applications, the magnitudes reported here should be interpreted as context-specific to the study area, while the key contribution lies in making the preference–feasibility mechanism explicit and empirically testable (Garcia-Prats et al., 2016).

A key boundary of the current framework is that biophysical and economic coefficients—yields, net irrigation requirements, input costs, and output prices—are held constant across SSPs, so that the results isolate the contribution of shifting social preferences to allocation outcomes while holding the production and market environment fixed. This is a deliberate modeling choice rather than an oversight, as it allows the preference–feasibility mechanism to be identified and stress-tested cleanly across normative layers. In practice, however, each SSP narrative implies a co-evolving technological, market, and climatic context. SSP1 would plausibly involve improved irrigation efficiency and more favorable input markets; SSP3 would likely compound scarcity with degraded infrastructure and greater price volatility; and SSP4 may deepen market segmentation in ways that alter crop profitability independently of normative steering. Holding coefficients constant therefore means that the welfare magnitudes reported here should be interpreted as preference-driven effects under a fixed feasibility frontier, and may understate the full divergence in welfare outcomes across SSPs once production conditions and market prices are allowed to vary. Future extensions should therefore couple the LP with SSP-consistent price trajectories and scenario-adjusted irrigation-efficiency parameters, so that the feasibility frontier itself becomes scenario-conditional rather than a shared baseline against which only preferences vary.

A related modeling boundary is that the LP assumes constant returns to scale and a risk-neutral objective. In reality, however, smallholder crop adoption in drought-prone settings is strongly shaped by risk aversion. A risk-sensitive formulation—such as a mean-variance or CVaR objective—would likely attenuate adoption of higher-return but more yield-volatile crops favored by the social weights, thereby creating a tractable tension between social-alignment incentives and household-level risk management. Future work should therefore examine how risk-adjusted objective functions interact with the Top-M alignment constraint, particularly for high-SEVI households.

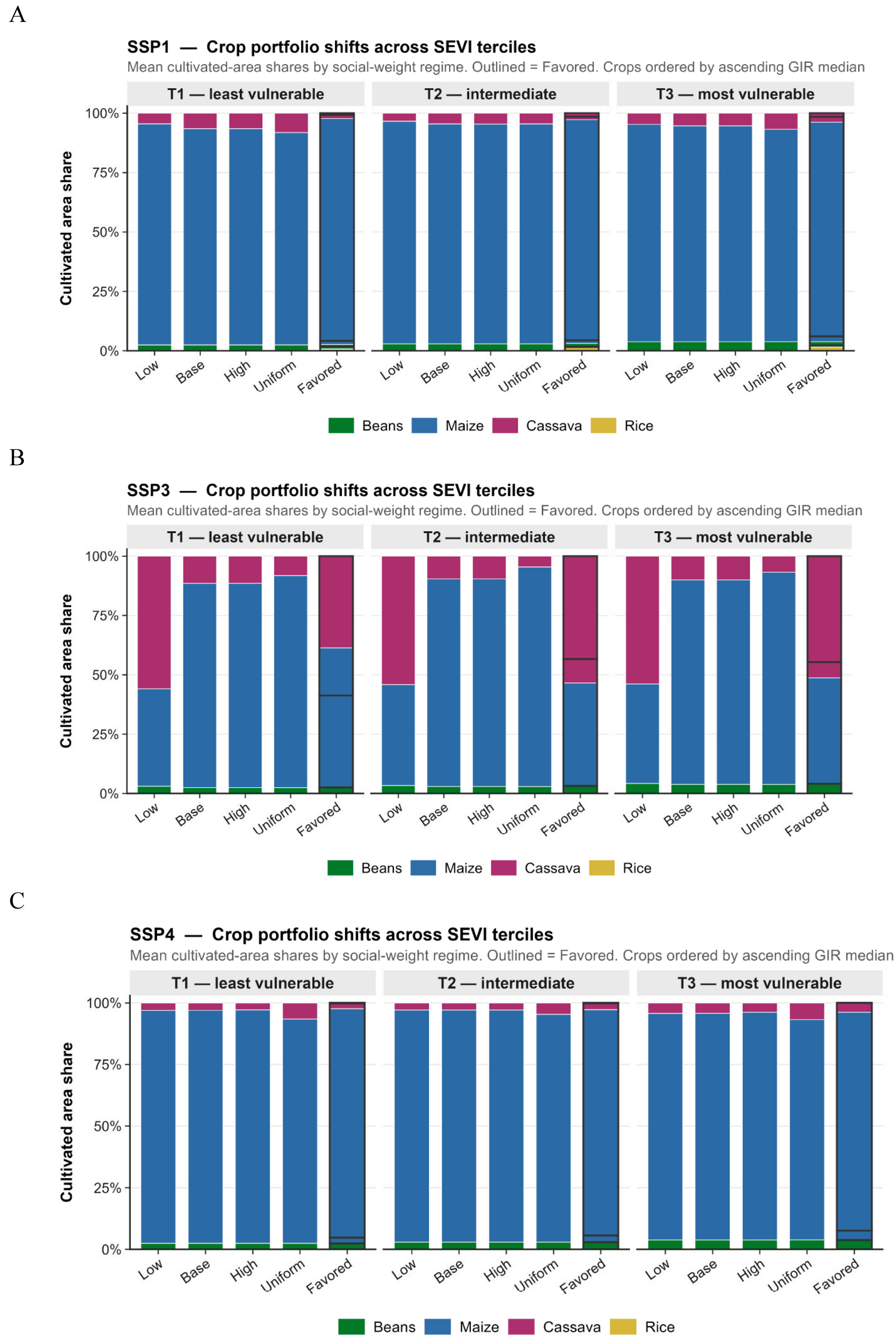

Fig. 10. Scenario-conditional crop portfolio responses across Socioeconomic Vulnerability Index (SEVI) terciles and social-weight layers (A: SSP1; B: SSP3; C: SSP4).

Our results also indicate that the tension between normative alignment and feasibility is not constant: it changes systematically with the scenario context and intensifies when scarcity compresses the household's feasible frontier. This scarcity-amplification mechanism is consistent with hydroeconomic evidence that the marginal value (shadow price) of additional water increases under scarcity and high-value uses, thereby magnifying the welfare implications of binding water constraints (Garcia-Prats et al., 2016). This linkage becomes analytically consequential once preferences are conditioned on Shared Socioeconomic Pathways (SSPs). SSPs were designed to represent futures that differ systematically in institutional capacity, market access, and adaptation challenges; conditioning preferences on SSPs therefore shifts them from a narrative add-on to a transparent stress-test device for decision support (O'Neill et al., 2017; Riahi et al., 2017). Under this logic, the same collective priority structure may remain "low-regret" when feasibility slack is ample yet become welfare-costly when scarcity binds more often. Operationally, this manifests as a threshold: increases in α_s or μ_s can improve alignment under enabling pathways, but under adverse SSPs they more readily push solutions toward less profitable margins or tighter constraints, signaling when normative steering requires complementary enabling investments (reliability, access, governance, and technology) to avoid private welfare losses. Recent SSP-based hydroeconomic WEFE assessments likewise show how system performance can remain acceptable under enabling pathways yet become highly constrained under adverse SSP, motivating adaptation packages rather than standalone steering (Pulido-Velazquez et al., 2025).

Relative to MCDA/AHP crop-planning studies, the contribution is not another ranking exercise but an operational bridge from prioritization to allocative implications under binding constraints. MCDA remains widely used because it provides a transparent elicitation structure, yet its outputs often remain as scores or ranks without quantifying what those priorities imply once water and other constraints determine the feasible set (Hajkowicz and Collins, 2007). Embedding $w_{s,k}$ within the LP transforms priorities into implementable portfolios and, crucially, reveals whether stronger alignment pressure (α_s) and social-reward monetization (μ_s) shift allocations with limited private cost or instead introduce feasibility tension. In consequence, the discussion moves from "which crop should be prioritized" to "which combination of priorities and constraints yields a viable portfolio"—and under which scenario conditions that viability can be sustained without transferring costs to households.

Placing this advance within the Colombian literature is important because integrated simulation–optimization is already established as a relevant direction for irrigation decision support. Terán-Chaves and Polo-Murcia (2021) coupled cropping-pattern simulation with optimization to improve water-use efficiency and economic returns in Colombia-relevant contexts, demonstrating the practical value of linking biophysical response and allocation. Building on that foundation, the present framework extends the state of practice by treating preferences as Bayesian, uncertainty-reporting inputs and by making them scenario-conditional and operationally accountable at the household decision scale. The novelty is therefore not "adding preferences," but disciplining them: representing disagreement explicitly, carrying it through optimization, and revealing where normative steering is feasible versus where it becomes costly without complementary measures.

A further contribution is credibility under heterogeneity. By allowing the biophysical module to generate household-specific coefficients consistent with process-based crop–water relationships, the optimizer is confronted with realistic within-crop variability rather than representative-farm averages. This matters because, under scarcity, heterogeneity determines which options become structurally unattractive for subsets of households and therefore which "preference-consistent" portfolios are actually implementable. In that sense, the framework aligns with AquaCrop's conceptual emphasis on process-consistent yield responses to water rather than ad hoc production functions, while remaining tractable for large-scale scenario exploration (Raes et al., 2009).

Internationally, the results connect to a broader hydro-economic insight from semi-arid regions with heterogeneous institutions: normative levers translate into welfare gains only if they remain compatible with the local constraint regime. Hydro-economic assessments in water-scarce basins have repeatedly shown that explicit constraints reveal trade-offs that ranking-only approaches tend to hide (Blanco-Gutiérrez et al., 2013). Beyond feasibility, however, feedbacks and second-order effects can reshape incentives and outcomes. Modular recursive hydro-micro-macro frameworks show that policy-induced land and water reallocations can propagate to market supply and prices, partially offsetting or amplifying profitability changes and generating non-linear land and water-use responses (Pérez-Blanco et al., 2022). Read in that light, the contribution here is a feasibility-grounded implementability test at the household scale, while the natural extension is to assess whether preference-consistent portfolios persist once prices, energy costs, or endogenous hydrologic dynamics feed back into profitability and water use (Pérez-Blanco et al., 2022; Ortiz-Partida et al., 2023; Pulido-Velazquez et al., 2025).

Treating preferences probabilistically also strengthens transferability. A recurring critique of stakeholder layers is subjectivity; defensibility improves when elicitation is protocol-driven and uncertainty is explicit rather than implicit. Reporting posteriors and credible intervals makes disagreement visible and decision-relevant, enabling sensitivity envelopes and targeted deliberation where priorities are contested, while supporting more confident use of robust priorities (Hemming et al., 2018a,b). Reliability and robustness should be interpreted as complementary diagnostics: uncertainty describes dispersion in judgments, while robustness describes stability of inferences under perturbations. Where reliability is reported, standard guidance supports using inter-rater measures such as ICC to contextualize agreement without implying unanimity (Koo and Li, 2016).

Finally, the distributional analysis underscores a key policy implication: preference-consistent targeting can credibly inform what is socially prioritized, but it does not automatically resolve capability constraints. When vulnerability gradients persist despite maintained alignment, the binding mechanism is not preference exclusion but a compressed feasible frontier—implicating interventions that expand feasibility for high-vulnerability households (credit, extension, irrigation access/efficiency, and enabling governance). This aligns with the broader water-productivity perspective: realized gains depend not only on agronomic potential but also on constraints and the capacity to adopt and operate within them (Zwart and Bastiaanssen, 2004). Translating this into operational terms, the enabling interventions can be grouped into three complementary tracks. The first is infrastructure investment. Colombia's Sistema Nacional de Adecuación de Tierras (SNAT) provides a policy vehicle for co-financing on-farm water storage and distribution upgrades; where SNAT resources have been channeled toward small-scale drip and sprinkler systems in semi-arid Caribbean departments, documented gains in water productivity have been on the order of 20–35% for maize and bean smallholders, directly relaxing the water constraint that binds most high-SEVI households in the present model. FAO-supported small-scale irrigation schemes in comparable semi-arid contexts in Latin America (e.g., Ecuador's Sierra and northeastern Brazil) show that even modest increases in reliable dry-season water access—equivalent to 15–30 mm cycle^{-1} above the household's baseline accessible depth—can shift households from the binding to the non-binding feasibility regime, enabling preference-consistent portfolios without private welfare loss. The second track is targeted credit. High-SEVI households in the Cesar Department currently face limited access to formal agricultural credit, which constrains both input purchases and the upfront cost of transitioning to socially preferred crops. Revolving credit lines linked to Colombia's DRR-agricultural instruments (Finagro and the Fondo Agropecuario de Garantías) offer a mechanism for financing drip irrigation adoption and input packages for cassava and bean diversification—the crops most consistently favored under SSP3's food-security-oriented social weights—without requiring collateral that subsistence households rarely hold. The third track is differentiated extension. The present results suggest that under SSP4 (Fair Market Access and Cooperative Marketing), the binding constraint for preference-consistent targeting is less often water availability than it is market access and price realization. This maps directly onto the SSP4-dominant strategy identified by stakeholders: extension services in this scenario should prioritize market linkage facilitation—cooperative marketing agreements, value chain integration for beans and cassava, and post-harvest handling—rather than purely agronomic advisory. Under SSP1 and SSP3, by contrast, the agronomic track dominates: deficit irrigation scheduling, crop-calendar optimization for dry-year conditions, and input-use efficiency are the bottlenecks that extension must address to make socially preferred portfolios privately viable.

A practical caution is that "efficiency" narratives can generate cross-domain impacts—most notably energy costs under modernization or pressurized systems—so normative steering should be interpreted alongside broader system implications to avoid unintended welfare transfers. Evidence from irrigation modernization shows that water savings and energy requirements can move in opposite directions, reshaping incentives and feasible crop choices (Tarjuelo et al., 2015). In SSP-like futures where scarcity binds more often, this strengthens the case for integrated policy design: preference-consistent portfolios may be implementable under enabling conditions, but constrained futures may require combined measures (water reliability plus affordability/energy-aware modernization and institutional support) to keep normative steering both feasible and equitable.

5. Conclusion

This study advances household-level hydro-economic optimization by moving beyond the representation of farmers as purely profit-maximizing agents and instead modeling them as decision-makers operating within binding social and climatic constraints. Participatory preferences are conditioned on SSP narratives and summarized as SSP-specific crop-preference weights (Bayesian posterior), which are operationalized in the linear program through a normative reward term and a Top-M alignment rule (Methods; Appendix 3). Results confirm the expected mechanism: increasing normative leverage raises the social component of the objective, whereas income responses depend on household feasibility—water, land, labor, and budget constraints—and on the SSP-conditioned preference signal. Under the calibrated alignment settings, feasibility is maintained and the alignment slack remains inactive in the benchmark runs, indicating that the elicited targets are implementable under the reference scarcity conditions. Future work should delineate feasibility boundaries by testing stricter alignment thresholds and alternative scarcity regimes.

Across SEVI terciles (Polo-Murcia et al., 2026), welfare differences are explained primarily by capability constraints rather than by exclusion from collective priorities. Net income declines sharply from low-to high-vulnerability households and water use falls in parallel, consistent with reduced capacity to convert endowments and available crop options into income under binding constraints. Importantly, realized Top-M area shares remain high across terciles, suggesting that the normative preference layer does not systematically disadvantage vulnerable households.

Policy implications follow directly. Posterior weights and their credible intervals can support transparent prioritization by distinguishing robust signals from contested ones. Normative levers $\left(\alpha_{s,g}, \mu_{s,g}\right)$ should be designed SSP-conditionally: preference-consistent targeting is low-regret where feasibility is relatively flexible (SSP1/SSP4), but it requires complementary enabling investments under constrained futures (SSP3). Reducing vulnerability therefore hinges on expanding feasibility for high-SEVI households—through improved irrigation access and efficiency, credit, extension, and enabling governance—so that socially preferred portfolios do not translate into private welfare losses. Concretely, infrastructure investment through SNAT co-financing mechanisms, revolving agricultural credit via Finagro and the Fondo Agropecuario de Garantías, and SSP-conditional extension services—emphasizing deficit irrigation scheduling under SSP1/SSP3 and cooperative market linkage under SSP4—constitute the three enabling tracks most directly aligned with the binding constraints identified in this study. Overall, the framework provides a practical route to embed participatory legitimacy and uncertainty into irrigation planning without sacrificing feasibility under benchmark scarcity.

Four directions merit priority in future research. First, the biophysical and economic coefficients—currently held constant across SSPs—should be coupled with SSP-consistent climate projections and price trajectories, so that the feasibility frontier itself becomes scenario-conditional rather than a shared baseline. Second, the Bayesian–LP architecture should be tested in other semi-arid smallholder basins in Latin America and Sub-Saharan Africa to assess which mechanisms generalize beyond the Cesar case. Third, dynamic multi-period optimization would extend the framework to capture crop rotation decisions and capital investment trajectories that single-period LPs cannot represent. Fourth, replacing the deterministic objective with a mean-variance or CVaR formulation would make explicit the tension between social-alignment incentives and household risk aversion—an interaction that is most consequential for high-SEVI households and for the yield-volatile crops that social weights tend to promote.

CRediT authorship contribution statement

Sonia Mercedes Polo-Murcia: Writing – review & editing, Writing – original draft, Visualization, Validation, Supervision, Software, Resources, Project administration, Methodology, Investigation, Funding acquisition, Formal analysis, Data curation, Conceptualization. **Marta García-Mollá:** Writing – review & editing, Writing – original draft, Supervision, Methodology, Investigation, Formal analysis, Conceptualization. **César Augusto Terán-Chaves:** Writing – review & editing, Writing – original draft, Visualization, Validation, Supervision, Software, Resources, Project administration, Methodology, Investigation, Funding acquisition, Formal analysis, Data curation, Conceptualization.

Data availability statement

The data that support the findings of this study are available from the author upon request.

Funding statement

This paper was developed within the framework of the project “Optimización del agua y uso eficiente del suelo para mejorar la producción agropecuaria en escenarios de vulnerabilidad agroclimática del departamento del Cesar”—BPIN 2017000100050—supported by the Colombian Fund for Science, Technology, and Innovation of General System Royalties (FCTeI-SGR), together with Gobernación del Cesar funds. Funding for open access charge: Universitat Politècnica de València.

Declaration of competing interest

The authors declare that they have no known competing financial interests or personal relationships that could have appeared to influence the work reported in this paper.

Acknowledgements

We would like to extend our thanks to the anonymous reviewers for their kind suggestions to improve this manuscript. Funding for open access charge: Universitat Politècnica de València.

Appendix A. Supplementary data

Supplementary data to this article can be found online at https://doi.org/10.1016/j.indic.2026.101254.

Data availability

Data will be made available on request.

References

Abdolalizadeh, E., Bakhoda, H., Almassi, M., 2025. Optimizing cultivation choices through the TOPSIS and conceptual models: expert insights on agricultural practices. Environ. Sustain. Indic. 27, 100780. https://doi.org/10.1016/j.indic.2025.100780.

Batool, D., Shahbaz, M., Asif, H.S., Shaukat, K., Alam, T.M., Hameed, I.A., Ramzan, Z., Waheed, A., Aljuaid, H., Luo, S., 2022. A hybrid approach to tea crop yield prediction using simulation models and machine learning. Plants 11 (15), 1925. https://doi.org/10.3390/plants11151925.

Blanco-Gutiérrez, I., Varela-Ortega, C., Purkey, D.R., 2013. Integrated assessment of policy interventions for promoting sustainable irrigation in semi-arid environments: a hydro-economic modeling approach. J. Environ. Manag. 128, 144–160. https://doi.org/10.1016/j.jenvman.2013.04.037.

Cai, X., McKinney, D.C., Lasdon, L.S., 2002. Integrated hydrologic-agronomic-economic model for river basin management. J. Water Resour. Plann. Manag. 129 (1), 4–17. https://doi.org/10.1061/(asce)0733-9496(2003)129:1(4.

Cao, Z., Zhu, T., Cai, X., Wang, J., Zhao, Y., Zhao, X., 2024. Hydroeconomic optimization of integrated water and salinity management in an arid agricultural region. J. Water Resour. Plann. Manag. 150 (10). https://doi.org/10.1061/jwrmd5.wreng-6098.

Chumbe, R., Silva, S., Garcia, Y., 2023. Comparison of the machine learning and AquaCrop models for quinoa crops. Res. Agric. Eng. 69 (2), 65–75. https://doi.org/10.17221/86/2021-rae.

Crespo, D., Nemati, M., Dinar, A., Frankel, Z., Halberg, N., 2025. Assessing the economic value of water in the colorado river basin: a hydroeconomic analysis. Water Resources And Economics, 100266. https://doi.org/10.1016/j.wre.2025.100266.

DANE. Departamento Nacional de Estadísticas, 2014. Censo nacional agropecuario. Available online: https://www.dane.gov.co/index.php/estadisticas-por-tema/agropecuario/censo-nacion. (Accessed 12 March 2025).

De Wit, A., Boogaard, H., Fumagalli, D., Janssen, S., Knapen, R., Van Kraalingen, D., Supit, I., Van Der Wijngaart, R., Van Diepen, K., 2018. 25 years of the WOFOST cropping systems model. Agric. Syst. 168, 154–167. https://doi.org/10.1016/j.agsy.2018.06.018.

Domínguez, A., Martínez-Romero, A., Leite, K., Tarjuelo, J., De Juan, J., López-Urrea, R., 2013. Combination of typical meteorological year with regulated deficit irrigation to improve the profitability of garlic growing in central Spain. Agric. Water Manag. 130, 154–167. https://doi.org/10.1016/j.agwat.2013.08.024.

Eamen, L., Brouwer, R., Razavi, S., 2022. Comparing the applicability of hydro-economic modelling approaches for large-scale decision-making in multi-sectoral and multi-regional river basins. Environ. Model. Software 152, 105385. https://doi.org/10.1016/j.envsoft.2022.105385.

Esteve, P., Varela-Ortega, C., Blanco-Gutiérrez, I., Downing, T.E., 2015. A hydro-economic model for the assessment of climate change impacts and adaptation in irrigated agriculture. Ecol. Econ. 120, 49–58. https://doi.org/10.1016/j.ecolecon.2015.09.017.

Foster, T., Brozović, N., Butler, A.P., Neale, C.M.U., Raes, D., Steduto, P., et al., 2017. AquaCrop-OS: an open source version of FAO's crop water productivity model. Agric. Water Manag. 181, 18–22.

Garcia-Prats, A., Del Campo, A.D., Pulido-Velazquez, M., 2016. A hydroeconomic modeling framework for optimal integrated management of forest and water. Water Resour. Res. 52 (10), 8277–8294. https://doi.org/10.1002/2015wr018273.

Hajkowicz, S., Collins, K., 2007. A review of multiple criteria analysis for water resource planning and management. Water Resour. Manag. 21, 1553–1566. https://doi.org/10.1007/s11269-006-9112-5.

Harou, J.J., Pulido-Velazquez, M., Rosenberg, D.E., Medellín-Azuara, J., Lund, J.R., Howitt, R.E., 2009. Hydro-economic models: concepts, design, applications, and future prospects. J. Hydrol. 375 (3–4), 627–643. https://doi.org/10.1016/j.jhydrol.2009.06.037.

Hayashi, K., 2000. Multicriteria analysis for agricultural resource management: a critical survey and future perspectives. Eur. J. Oper. Res. 122 (2), 486–500. https://doi.org/10.1016/s0377-2217(99)00249-0.

Hemming, V., Walshe, T.V., Hanea, A.M., Fidler, F., Burgman, M.A., 2018a. Eliciting improved quantitative judgements using the IDEA protocol: a case study in natural resource management. PLoS One 13 (6), e0198468. https://doi.org/10.1371/journal.pone.0198468.

Hemming, V., Burgman, M.A., Hanea, A.M., McBride, M.F., Wintle, B.C., 2018b. A practical guide to structured expert elicitation using the IDEA protocol. Methods Ecol. Evol. 9 (1), 169–180.

Holzworth, D.P., Huth, N.I., deVoil, P.G., Zurcher, E.J., Herrmann, N.I., McLean, G., Chenu, K., Van Oosterom, E.J., Snow, V., Murphy, C., Moore, A.D., Brown, H., Whish, J.P., Verrall, S., Fainges, J., Bell, L.W., Peake, A.S., Poulton, P.L., Hochman, Z., Keating, B.A., 2014. APSIM – evolution towards a new generation of agricultural systems simulation. Environ. Model. Software 62, 327–350. https://doi.org/10.1016/j.envsoft.2014.07.009.

Javan, K., Darestani, M., 2024. Assessing environmental sustainability of a vital crop in a critical region: investigating climate change impacts on agriculture using the SWAT model and HWA method. Heliyon 10 (3), e25326. https://doi.org/10.1016/j.heliyon.2024.e25326.

Javan, K., Lialestani, M.R.F.H., Ashouri, H., Moosavian, N., 2015. Assessment of the impacts of nonstationarity on watershed runoff using artificial neural networks: a case study in Ardebil, Iran. Model. Earth Syst. Environ. 1 (3). https://doi.org/10.1007/s40808-015-0030-5.

Jones, J., Hoogenboom, G., Porter, C., Boote, K., Batchelor, W., Hunt, L., Wilkens, P., Singh, U., Gijsman, A., Ritchie, J., 2003. The DSSAT cropping system model. Eur. J. Agron. 18 (3–4), 235–265. https://doi.org/10.1016/s1161-0301(02)00107-7.

Koo, T.K., Li, M.Y., 2016. A guideline of selecting and reporting intraclass correlation coefficients for reliability research. J. Chiropract. Med. 15 (2), 155–163. https://doi.org/10.1016/j.jcm.2016.02.012.

Montazar, A., Gaffari, A., 2011. An AHP model for crop planning within irrigation command areas. Irrig. Drain. 61 (2), 168–177. https://doi.org/10.1002/ird.645.

Ortega-Reig, M., García-Mollá, M., Sanchis-Ibor, C., Pulido-Velázquez, M., Girard, C., Marcos, P., Ruiz-Rodríguez, M., García-Prats, A., 2019. Adaptación de la agricultura a escenarios de cambio global. Aplicación de métodos participativos en la cuenca del río Júcar (España). Economía Agraria y Recursos Naturales 18 (2), 29. https://doi.org/10.7201/earn.2018.02.02.

Ortiz-Partida, J.P., Fernandez-Bou, A.S., Maskey, M., Rodríguez-Flores, J.M., Medellín-Azuara, J., Sandoval-Solis, S., Ermolieva, T., Kanavas, Z., Sahu, R.K., Wada, Y., Kahil, T., 2023. Hydro-economic modeling of water resources management challenges: current applications and future directions. Water Economics And Policy 9 (1). https://doi.org/10.1142/s2382624x23400039.

O'Neill, B.C., Kriegler, E., Ebi, K.L., Kemp-Benedict, E., Riahi, K., Rothman, D.S., van Ruijven, B.J., van Vuuren, D.P., Birkmann, J., Kok, K., Levy, M., Solecki, W., 2017. The roads ahead: narratives for shared socioeconomic pathways describing world futures in the 21st century. Glob. Environ. Change 42, 169–180. https://doi.org/10.1016/j.gloenvcha.2015.01.004.

Pérez-Blanco, C.D., Parrado, R., Essenfelder, A.H., Bodoque, J., Gil-García, L., Gutiérrez-Martín, C., Ladera, J., Standardi, G., 2022. Assessing farmers' adaptation responses to water conservation policies through modular recursive hydro-micro-macro-economic modeling. J. Clean. Prod. 360, 132208. https://doi.org/10.1016/j.jclepro.2022.132208.

Polo-Murcia, S.M., García-Mollá, M., Duarte-Carvajalino, J.M., Terán-Chaves, C.A., 2025. Multi-model approach using GIS-AHP, regional FDC modelling and AquaCrop-OS to support irrigation and enhance food security in Colombia. Hydrol. Sci. J. 1–23. https://doi.org/10.1080/02626667.2025.2551885.

Polo-Murcia, S.M., García-Mollá, M., Terán-Chaves, C.A., 2026. When vulnerability becomes strategy: a stakeholder-driven approach to climate adaptation in colombia's dry Caribbean.

Psomas, A., Vryzidis, I., Spyridakos, A., Mimikou, M., 2018. MCDA approach for agricultural water management in the context of water–energy–land–food nexus. Oper. Res. 21 (1), 689–723. https://doi.org/10.1007/s12351-018-0436-8.

Puig, F., Garcia-Vila, M., Soriano, M., Rodríguez-Díaz, J., 2025. AquaCrop-IoT: a smart irrigation platform integrating real-time images and weather forecasting. Comput. Electron. Agric. 235, 110372. https://doi.org/10.1016/j.compag.2025.110372.

Pulido-Velazquez, M., Macian-Sorribes, H., de León Pérez, D., Carricondo-Anton, J.M., Martinez-Capel, F., Garcia-Prats, A., Frances-Garcia, F., 2025. Assessment of climate change impacts on the water-energy-food-ecosystems (WEFE) nexus in the Jucar River Basin (Spain) using hydroeconomic and ecological modelling, and continental-scale economic projections. EGU General Assembly 2025. https://doi.org/10.5194/egusphere-egu25-16755. Vienna, Austria, 27 Apr–2 May 2025, EGU25-16755.

Radmehr, A., Bozorg-Haddad, O., Loáiciga, H.A., 2022. Integrated strategic planning and multi-criteria decision-making framework with its application to agricultural water management. Sci. Rep. 12 (1), 8406. https://doi.org/10.1038/s41598-022-12194-5.

Raes, D., Steduto, P., Hsiao, T.C., Fereres, E., 2009. AquaCrop – The FAO crop-water productivity model to simulate yield response to water: II. Main algorithms and software description. Agricultural Water Management 96 (4), 564–576.

Raes, D., Steduto, P., Hsiao, T.C., Fereres, E., 2018. Chapter 1: FAO crop-water Productivity Model to Simulate Yield Response to Water: Aquacrop: Version 6.0-6.1: Reference Manu*al. Rome: FAO,* 2018b. 19p.

Ramesh, V., Kumaresan, P., 2025. Stacked ensemble model for accurate crop yield prediction using machine learning techniques. Environ. Res. Commun. 7 (3), 035006. https://doi.org/10.1088/2515-7620/adb9c0.

Razavi, S., Duffy, A., Eamen, L., Jakeman, A.J., Jardine, T.D., Wheater, H., Hunt, R.J., Maier, H.R., Abdelhamed, M.S., Ghoreishi, M., Gupta, H., Döll, P., Moallemi, E.A., Yassin, F., Strickert, G., Nabavi, E., Mai, J., Li, Y., Thériault, J.M., Grimm, V., 2025. Convergent and transdisciplinary integration: on the future of integrated modeling of human-water systems. Water Resour. Res. 61 (2). https://doi.org/10.1029/2024wr038088.

Riahi, K., Van Vuuren, D.P., Kriegler, E., Edmonds, J., O'Neill, B.C., Fujimori, S., Bauer, N., Calvin, K., Dellink, R., Fricko, O., Lutz, W., Popp, A., Cuaresma, J.C., Kc, S., Leimbach, M., Jiang, L., Kram, T., Rao, S., Emmerling, J., Tavoni, M., 2017. The shared socioeconomic pathways and their energy, land use, and greenhouse gas emissions implications: an overview. Glob. Environ. Change 42, 153–168. https://doi.org/10.1016/j.gloenvcha.2016.05.009.

Sharafi, M., Behmanesh, J., Rezavardinejad, V., Samadianfard, S., 2023. Evaluation of AquaCrop and intelligent models in predicting yield and biomass values of wheat. Int. J. Biometeorol. 67 (4), 621–632. https://doi.org/10.1007/s00484-023-02440-4.

Tarjuelo, J.M., Rodriguez-Diaz, J.A., Abadía, R., Camacho, E., Rocamora, C., Moreno, M. A., 2015. Efficient water and energy use in irrigation modernization: lessons from Spanish case studies. Agric. Water Manag. 162, 67–77. https://doi.org/10.1016/j.agwat.2015.08.009.

Terán-Chaves, C.A., Polo-Murcia, S.M., 2021. Cropping pattern simulation-optimization model for water use efficiency and economic return. J. Agric. Eng. 52 (4). https://doi.org/10.4081/jae.2021.1197.

Terán-Chaves, C.A., Duarte-Carvajalino, J.M., Ipaz-Cuastumal, C., Vega-Amante, A., Polo-Murcia, S.M., 2023. Assessing the vulnerability of maize crop productivity to precipitation anomalies: a case study in the semiarid region of Cesar, Colombia. Water 15 (11), 2108. https://doi.org/10.3390/w15112108.

Ward, F.A., 2024. Hydroeconomic analysis: history, status, and possibilities. Water Economics And Policy 10 (4). https://doi.org/10.1142/s2382624x24300032.

Williams, N.J.R., Jones, N.C.A., Kiniry, N.J.R., Spanel, N.D.A., 1989. The EPIC crop growth model. Transactions Of The ASAE 32 (2), 497–511. https://doi.org/10.13031/2013.31032.

Wilson, K.J., Elfadaly, F.G., Garthwaite, P.H., Oakley, J.E., 2021. Recent advances in the elicitation of uncertainty distributions from experts for multinomial probabilities. In: Hanea, A.M., Nane, G.F., Bedford, T., French, S. (Eds.), Expert Judgement in Risk and Decision Analysis, International Series in Operations Research & Management Science, vol. 293. Springer, Cham. https://doi.org/10.1007/978-3-030-46474-5_2.

Yamane, T., 1973. Statistics: an Introductory Analysis. https://scholar.google.com/scholar_lookup?title=Statistics%3A%20An%20Introduction%20Analysis&publication_year=1967&author=T.%20Yamane.

Yet, B., Tuncer Şakar, C., 2020. Estimating criteria weight distributions in multiple criteria decision making: a Bayesian approach. Ann. Oper. Res. 293, 495–519. https://doi.org/10.1007/s10479-019-03313-z.

Zhang, J., Lin, X., Jiang, C., Hu, X., Liu, B., Liu, L., Xiao, L., Zhu, Y., Cao, W., Tang, L., 2024. Predicting rice phenology across China by integrating crop phenology model and machine learning. Sci. Total Environ. 951, 175585. https://doi.org/10.1016/j.scitotenv.2024.175585.

Zhou, H., Zhang, J., Cui, S., Zhao, J., 2023. Modeling hydrologic–economic interactions for sustainable development: a case study in Inner Mongolia, China. Sustainability 16 (1), 345. https://doi.org/10.3390/su16010345.

Zwart, S.J., Bastiaanssen, W.G., 2004. Review of measured crop water productivity values for irrigated wheat, rice, cotton and maize. Agric. Water Manag. 69 (2), 115–133. https://doi.org/10.1016/j.agwat.2004.04.007.